The University of Adelaide

School of Chemical Engineering

Cooperative Research Centre for Clean Power from Lignite

Physical Modelling of Mixing Between Rectangular Jets Present in Tangentially Fired Brown Coal Boilers

Ph.D. Thesis

Alessio Angelo Scarsella

Appendix A

A Calculation Methodology and Example of Determination of Experimental Flow Rates

A.1 Proposed Experimental Flow Rates

A sample calculation of the procedure used is outlined below with all the proposed flow rates for the experimental programs in order to carry out the flow visualisation for the rectangular nozzles. The primary jet velocity was fixed to maintain a Reynolds number of 10,000, the secondary jet flow rates will be manipulated according to the velocity ratios.

A.1.1 Determination of Secondary to Primary Velocity Ratio in one of the Yallourn 'W' Boilers

The objective of this section is to outline the calculation methodology used to determine the velocity ratio at which the boilers operate. The following block diagram (Figure A.1) is a schematic representation of the coal feed, milling and flue gas re-cycling system of one of the Yallourn 'W' boilers. Measured and calculated flow rates are tabulated in Table A.1 following the data of Simpson and McIntosh (1998). Table A.2 shows the flue gas composition from the same reference. Table A.3 shows the ultimate analysis of raw Morwell coal (Durie, 1991).

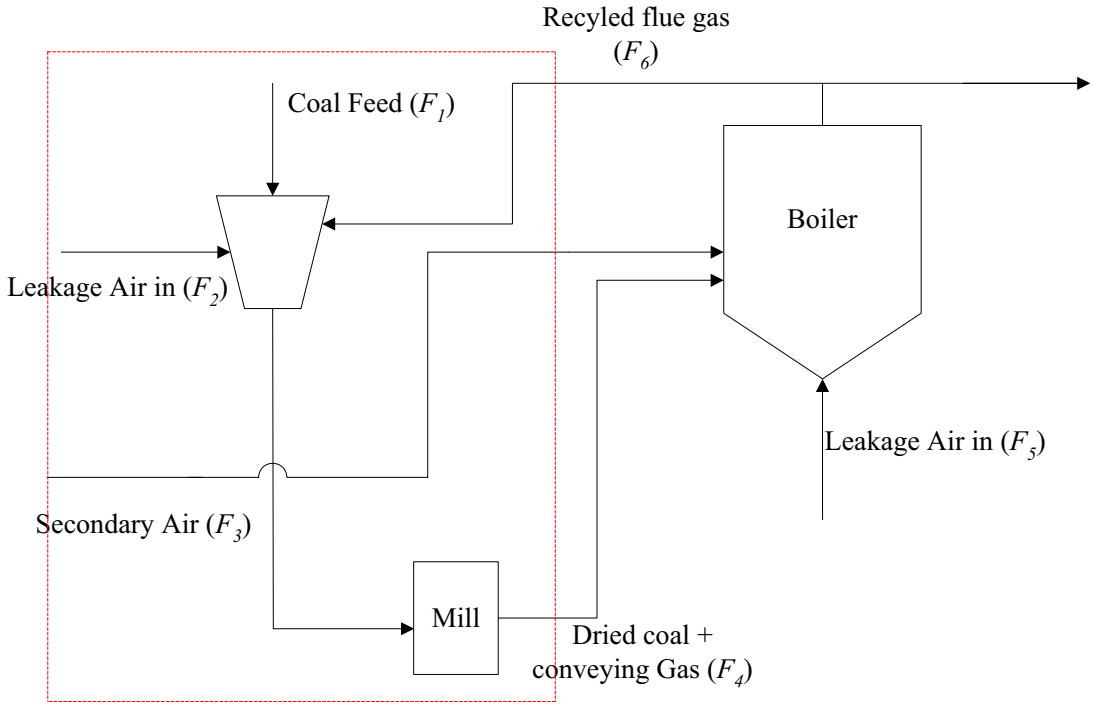

Figure A.1: Block diagram of coal conveying process in the Yallourn Power station**.**

Stream	Flow, tph	Temperature, C
F_1	576	15
F_2	131	15
F_3	1476	300
F_4	1368	120
F_5	633	15
F_6	889	1000

Table A. 1: Operating Flow rates of coal feed system to Yallourn 'W' Boilers.

Component	%(w/w)
CO_2	17.60%
H_2O	17.22%
SO_2	0.03%
O_2	4.72%
N_2	60.43%

Table A. 2: Flue gas composition.

Component	%w/w
C	22.31%
H	1.56%
O	9.19%
N	0.18%
S	0.08%
H_20	66.00%
Ash	0.65%

Table A. 3: Composition of Morwell raw coal (Durie, 1991).

The amount of flue gas required to heat the coal to 120°C and reduce the coal moisture to 15 % in the mill was calculated by delineating a control volume and performing mass and energy balances around the coal feeder and milling section.

The mass balance around this section is;

$$F_4 = F_1 + F_2 + F_6$$ **Equation A. 1**

The energy balance around this section is assumed to be adiabatic with only one phase change, that of the vaporised water from the de-watered coal,

$$F_4\left(\sum x_i \int_{T_{ref}}^{T} Cp_i(T)dT\right)_4 + \dot{m}_{H_20,vap}\Delta\hat{H}_{vap} = F_1\left(\sum x_i \int_{T_{ref}}^{T} Cp_i(T)dT\right)_1 + F_2\left(\sum x_i \int_{T_{ref}}^{T} Cp_i(T)dT\right)_2 + F_6\left(\sum x_i \int_{T_{ref}}^{T} Cp_i(T)dT\right)_6$$ **Equation A. 2**

where x_i is the mass fraction of the i^{th} component in the j^{th} stream, C_{pi} is the specific heat of the i^{th} component, T is temperature, $\Delta\hat{H}_{vap}$ is the enthalpy of vaporisation of water and $\dot{m}_{H_20,vap}$ is the mass of water vaporised per unit time from the wet coal, which was calculated to be;

$$\dot{m}_{H_20,vap} = \frac{F_1\left(x^1{}_{H_2O} - x^4{}_{H_2O}\right)}{\left(x^1{}_{H_2O} - x^4{}_{H_2O}\right)} = \frac{576*(0.66-0.15)}{1-0.15} = 345.6\_tph,$$

The value of $\dot{m}_{H_2O,Vap}$ can be inserted into Equation A.2, which can be combined with Equation A.1 to solve for the two unknowns F_4 and F_6.

The split of coal between main and vapour burners is assumed to be 80:20 whilst the split of gas is assumed to be 38:62 (Simpson and McIntosh, 1998). Hence the total flow rate of fuel to the main burners is 703 tph. The volumetric flow rate of this stream was determined with the use of the apparent density for a two phase system rather than the absolute density;

$$\rho_{app} = \frac{m_{solid} + m_{gas}}{V_{gas}} \qquad \textbf{Equation A. 3}$$

$$Q_{primary} = \frac{\dot{m}_{primary}}{\rho_{app}} = 243 \text{ m}^3/\text{s}$$

The total area of the main primary burners is 13.74 m^2 (12 primary burners in the main burner section) the calculated velocity was then found to be 17.71 m/s.

Table A.4 reports four different secondary air velocities and velocity ratios that were measured at various times at the plant. All four values are shown to demonstrate the range of plant operating conditions at a given primary flow. The total secondary air flow is reduced slightly from measured values since approximately 5% is used as core and cooling air in the primary burners.

Mass flow rate, kg/s	Volumetric flow-rate, m^3/s	Secondary velocity, m/s	Secondary to primary velocity ratio, λ
416	678.07	44.35	2.82
361	589.23	38.53	2.56
358	584.24	38.21	2.56
372	607.36	39.72	2.677

Table A. 4: Operating secondary flow-rates, velocities and velocity ratios.

A.1.2 Determination of Experimental Flow Rates.

The experimental velocity ratios were spread around the typical operating value found in the Yallourn boilers (Table 3.3). The experimental flow rates for primary and secondary jets were chosen so that the primary Reynolds number was fully turbulent at Re = 10,000. This equates to a primary flow rate of 8.21 L/min water.

Velocity ratio λ	Secondary velocity, m/s	Secondary Flow L/min
0	0.00	0.00
0.5	0.21	4.62
1.4	0.59	12.94
2.8	1.19	25.87
3.6	1.54	33.26
∞	0.57	12.31

Table A.5: Experimental secondary jet flow rates.

Appendix B

B Cross Stream Concentration of the Primary and Secondary Jet

This appendix illustrates the complete set of cross stream data in the *y* and *z* directions for the primary jet at velocity ratios of 0, 0.55, 1.4, 2.8 and 3.6, the secondary jet at velocity ratios of 0.55, 1.4, 2.8 and 3.6 at axial stations of *x/D* =0.1, 0.2, 0.5, 1, 2, 4, 6 and 8.

B.1 Primary Jet Cross Stream Normalised Concentration

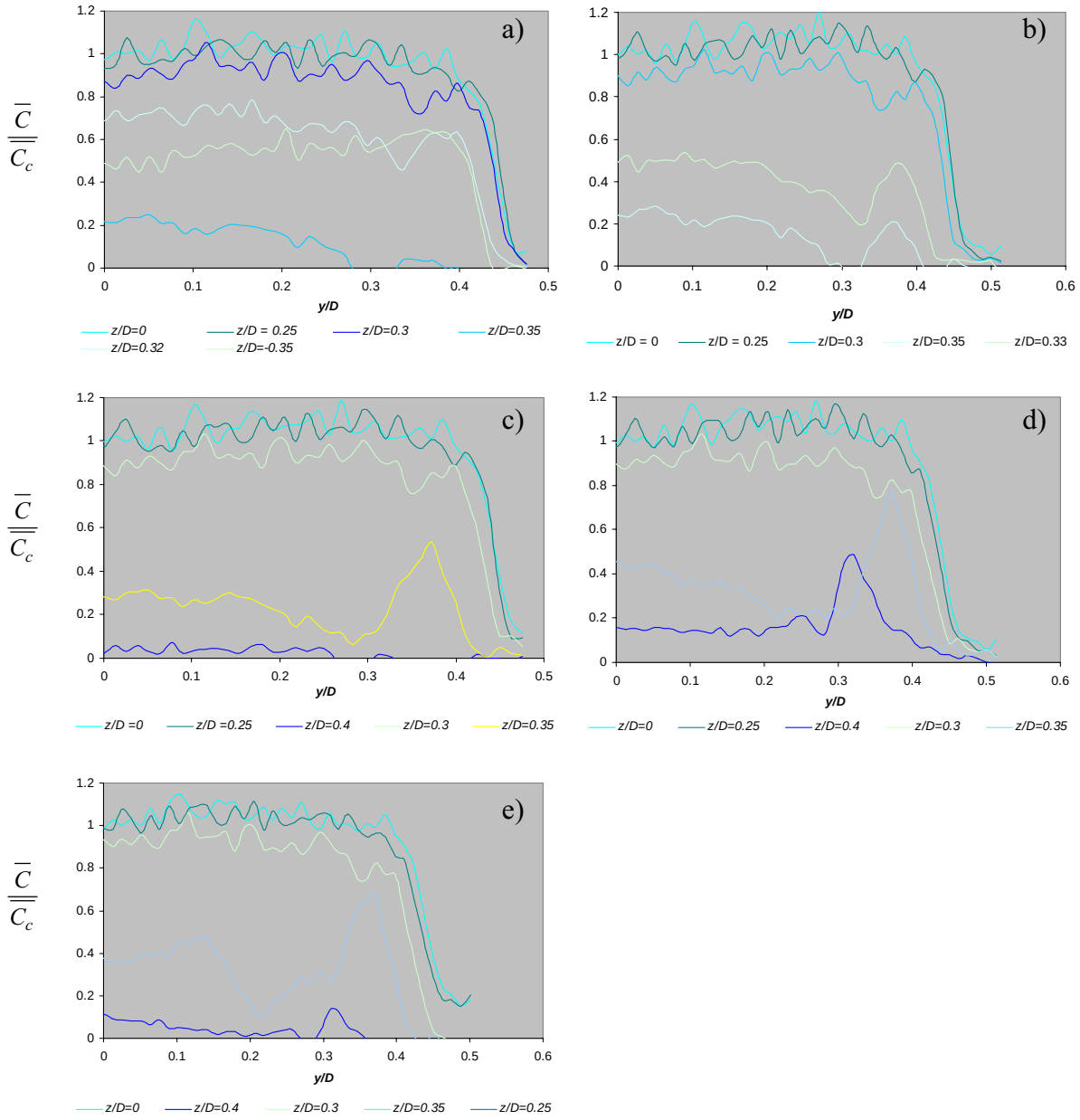

Figure B. 1: Normalised Concentration of the primary jet versus *y/D* through different *z/D* planes, at *x/D* =0.1, a) λ=0, b) λ=0.55, c) λ=1.4, d) λ=2.8, e) λ=3.6.

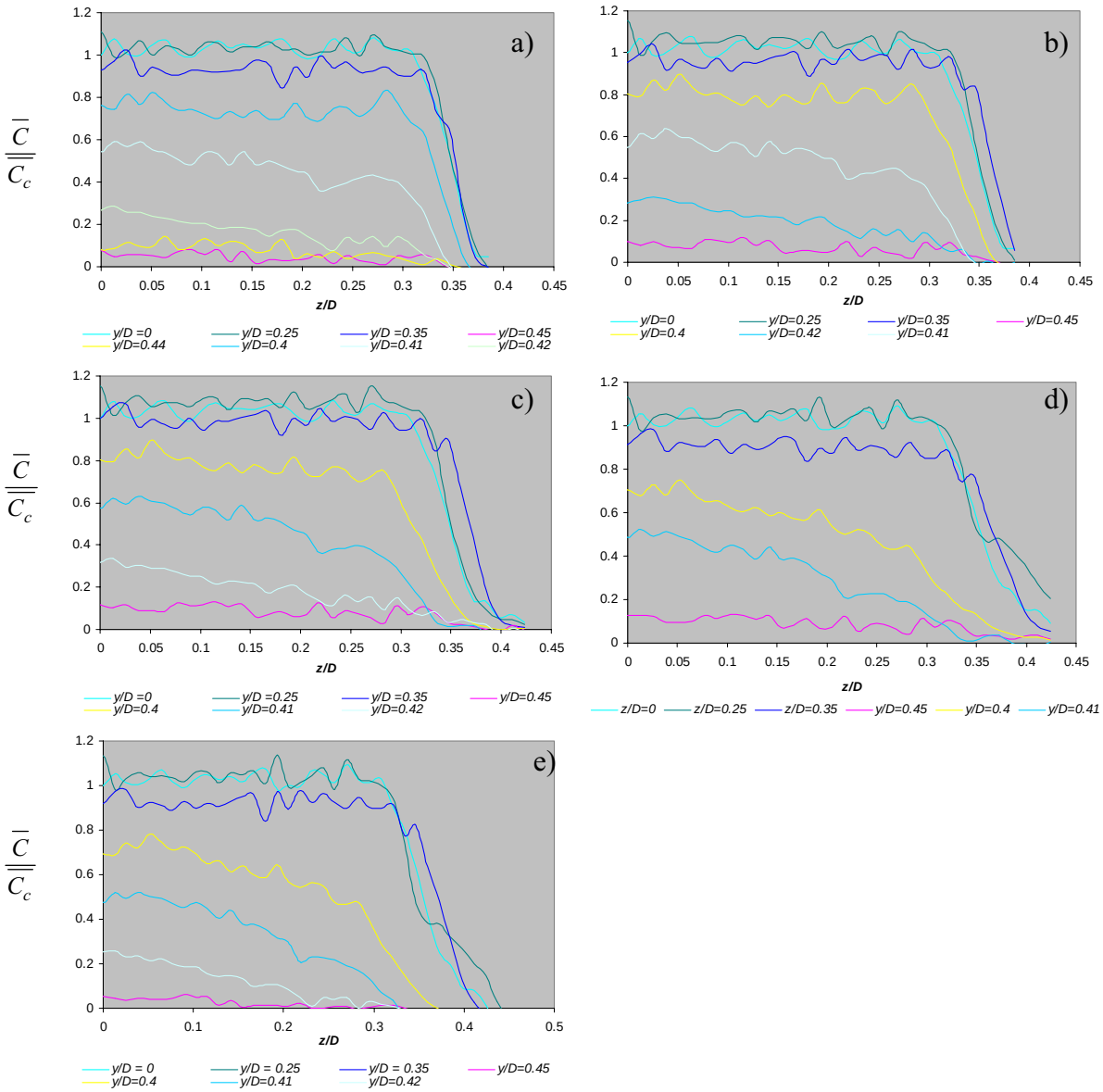

Figure B. 2: Normalised Concentration of the primary jet versus *z/D* through different *y/D* planes, at *x/D* =0.1, a) λ=0, b) λ=0.55, c) λ=1.4, d) λ=2.8, e) λ=3.6.

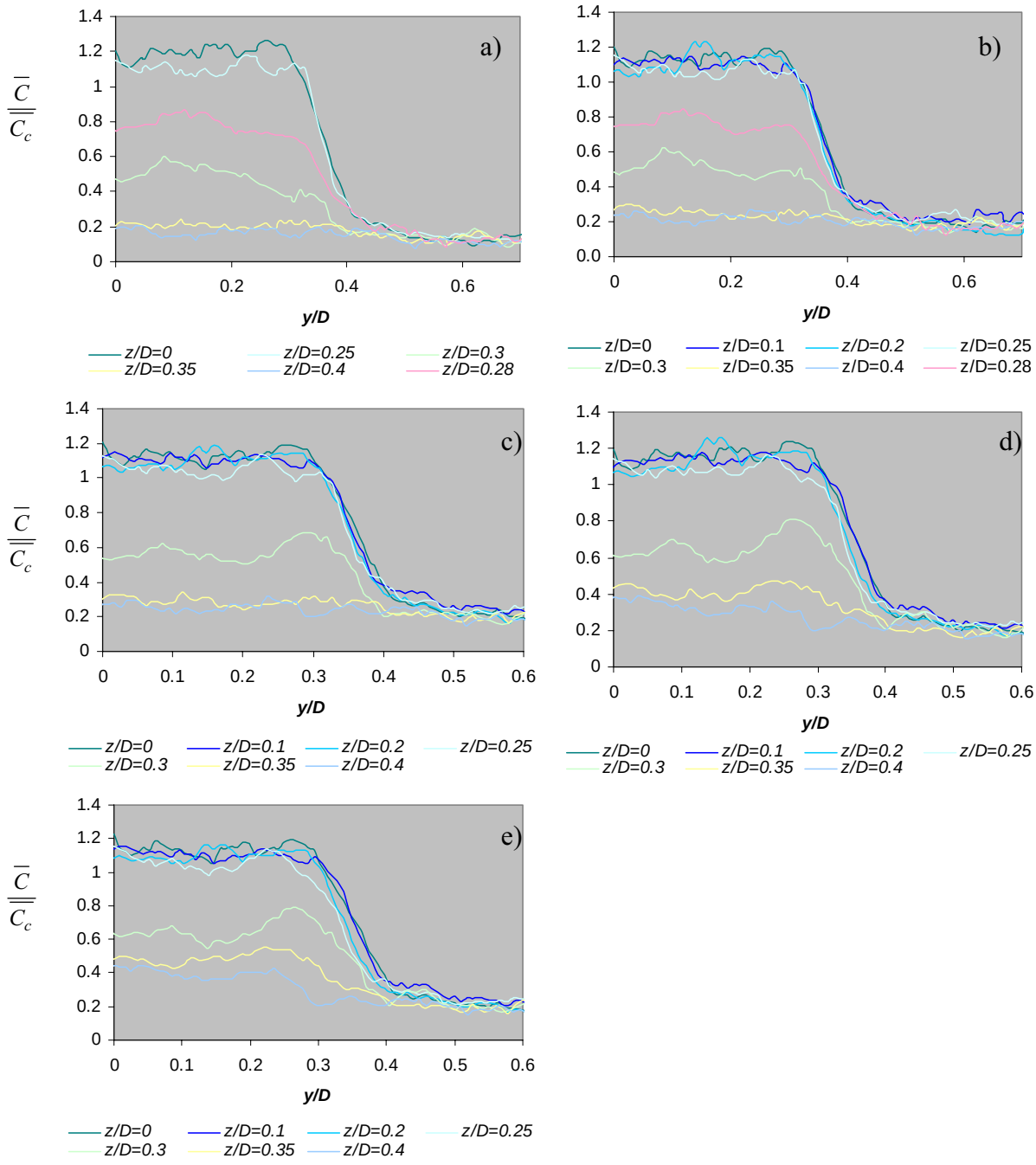

Figure B. 3: Normalised Concentration of the primary jet versus *y/D* through different *z/D* planes, at *x/D* =0.2, a) λ=0, b) λ=0.55, c) λ=1.4, d) λ=2.8, e) λ=3.6.

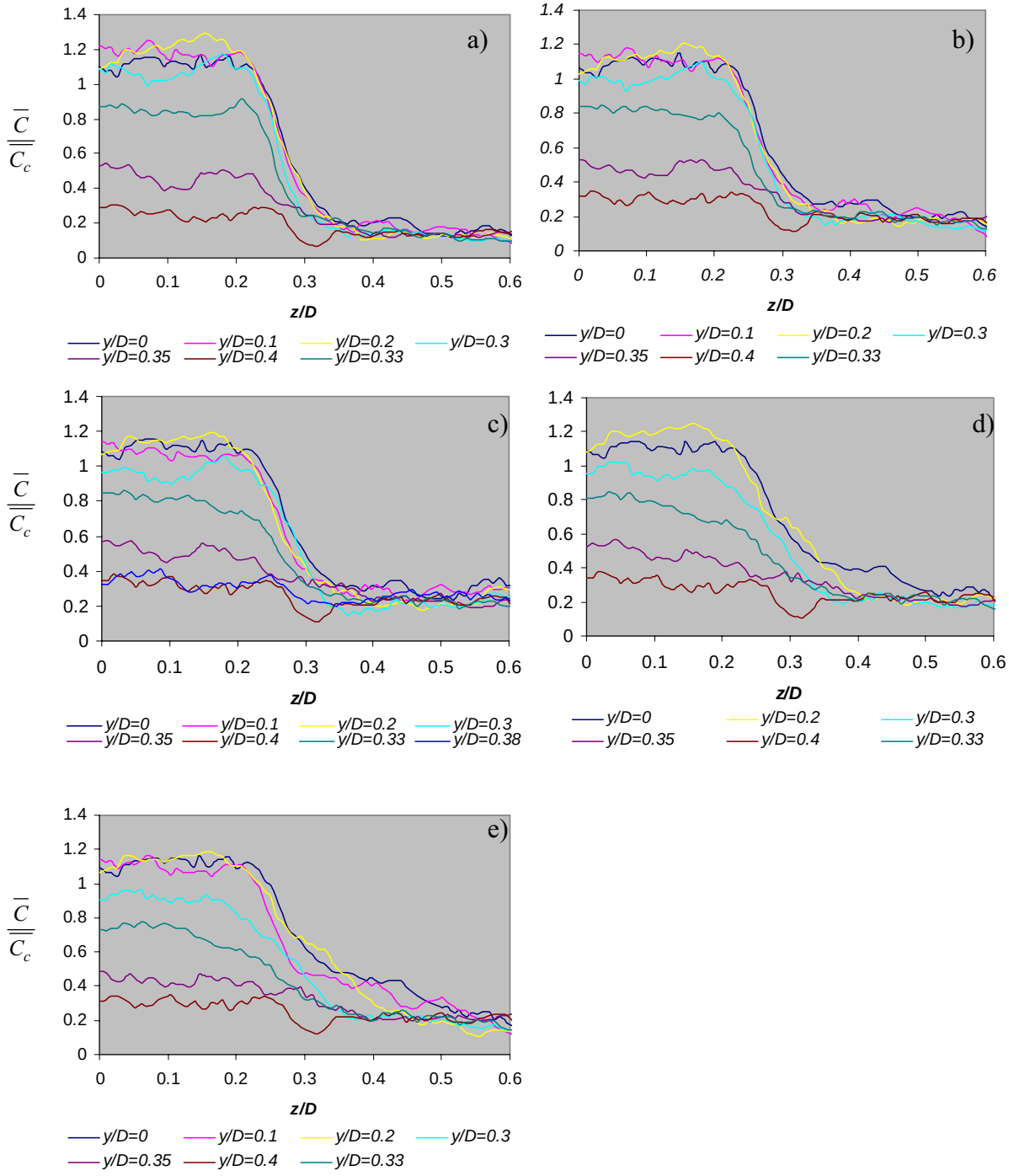

Figure B. 4: Normalised Concentration of the primary jet versus *z/D* through different *y/D* planes, at *x/D* =0.2, a) λ=0, b) λ=0.55, c) λ=1.4, d) λ=2.8, e) λ=3.6.

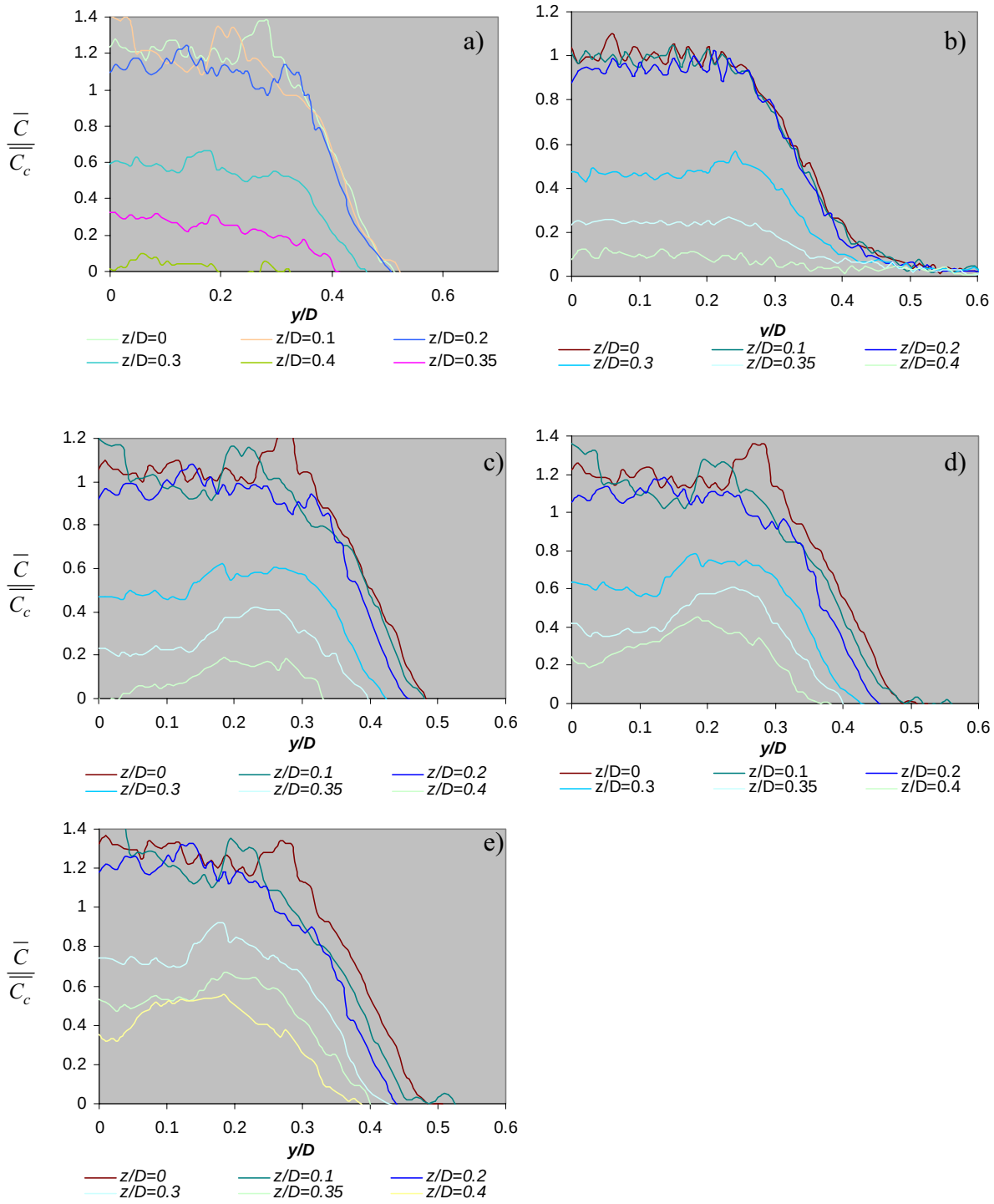

Figure B. 5: Normalised Concentration of the primary jet versus *y/D* through different *z/D* planes, at *x/D* =0.5, a) λ=0, b) λ=0.55, c) λ=1.4, d) λ=2.8, e) λ=3.6.

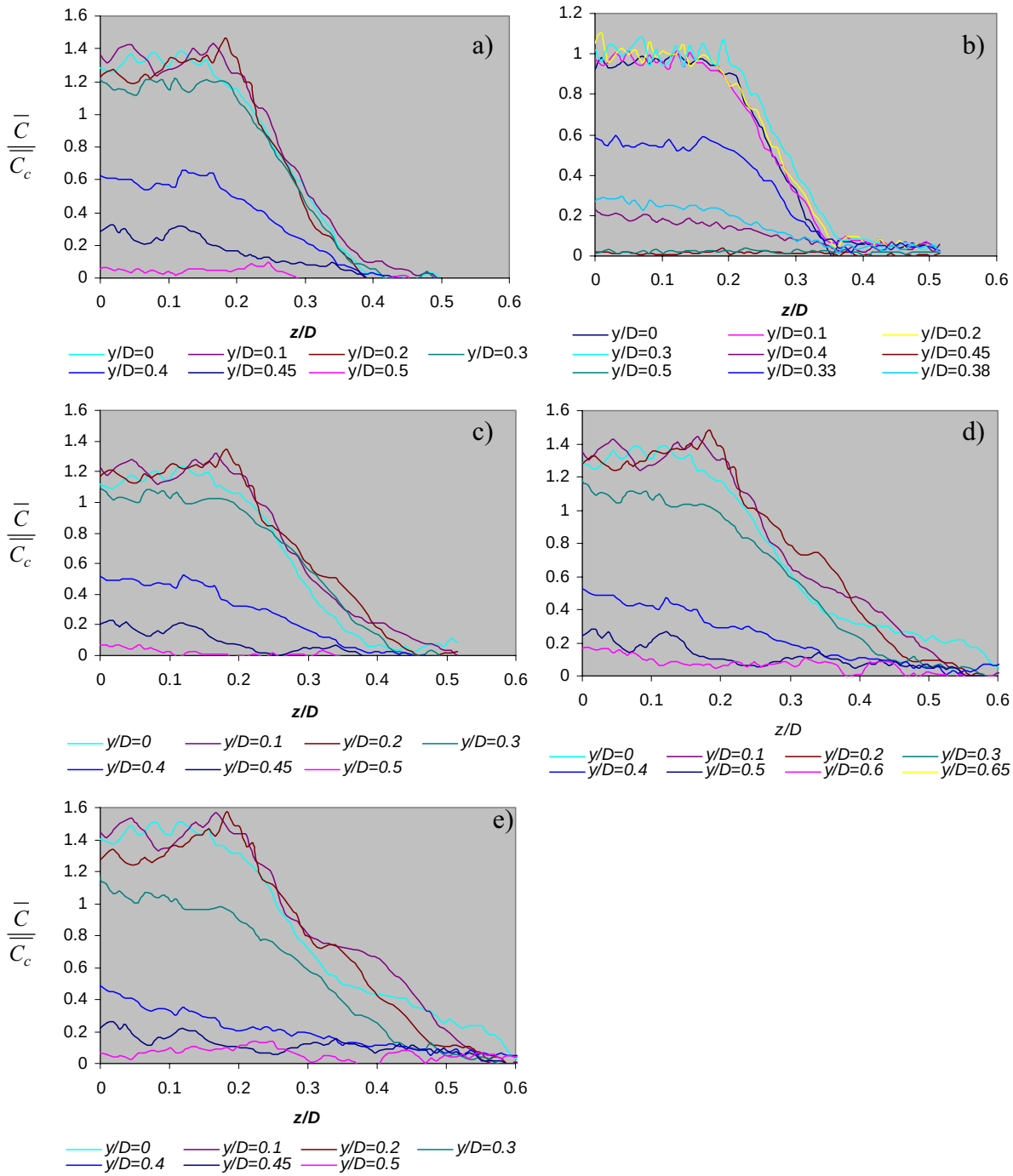

Figure B. 6: Normalised Concentration of the primary jet versus *z/D* through different *y/D* planes, at *x/D* =0.5, a) λ=0, b) λ=0.55, c) λ=1.4, d) λ=2.8, e) λ=3.6.

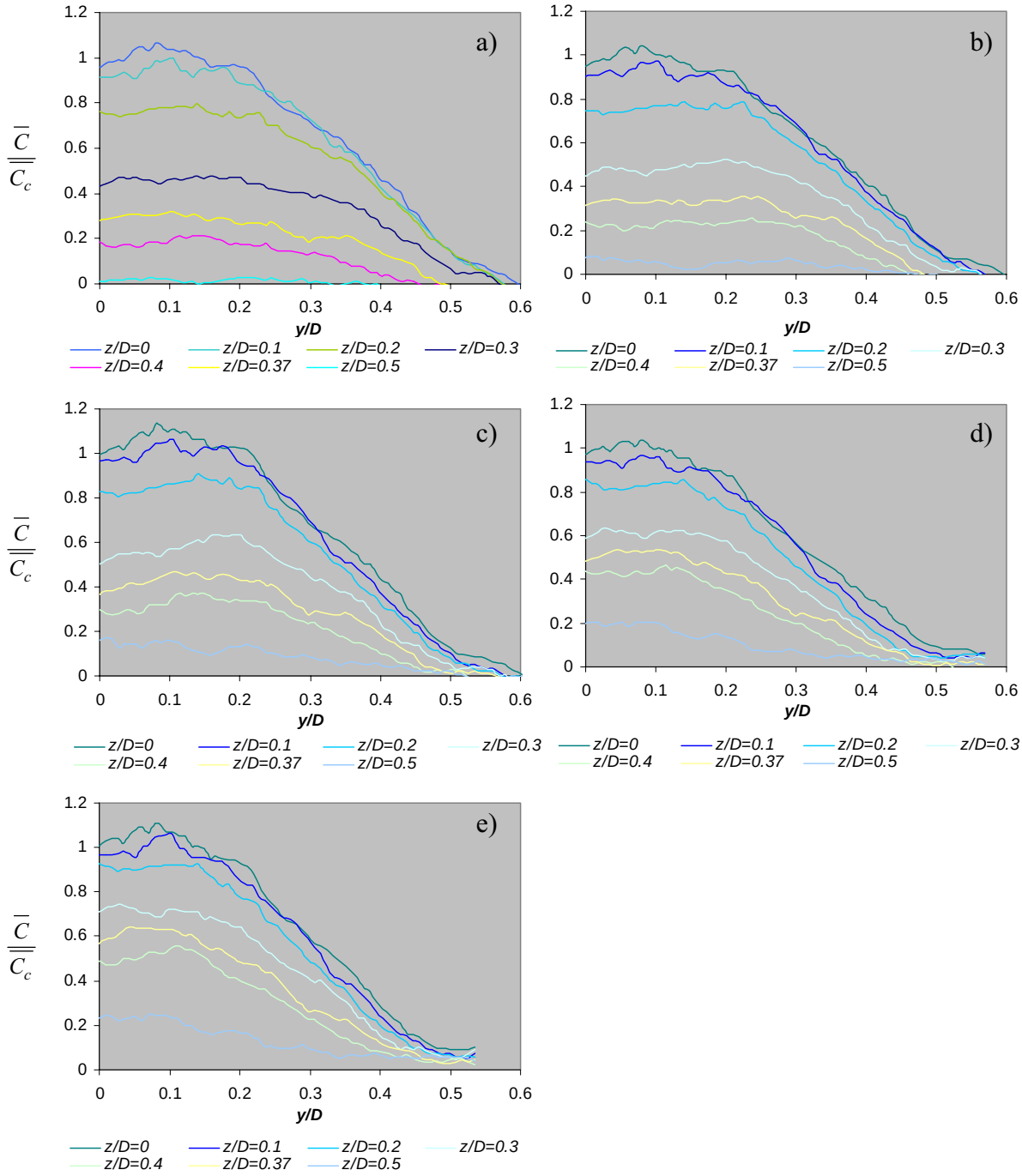

Figure B. 7: Normalised Concentration of the primary jet versus *y/D* through different *z/D* planes, at *x/D* =1, a) λ=0, b) λ=0.55, c) λ=1.4, d) λ=2.8, e) λ=3.6.

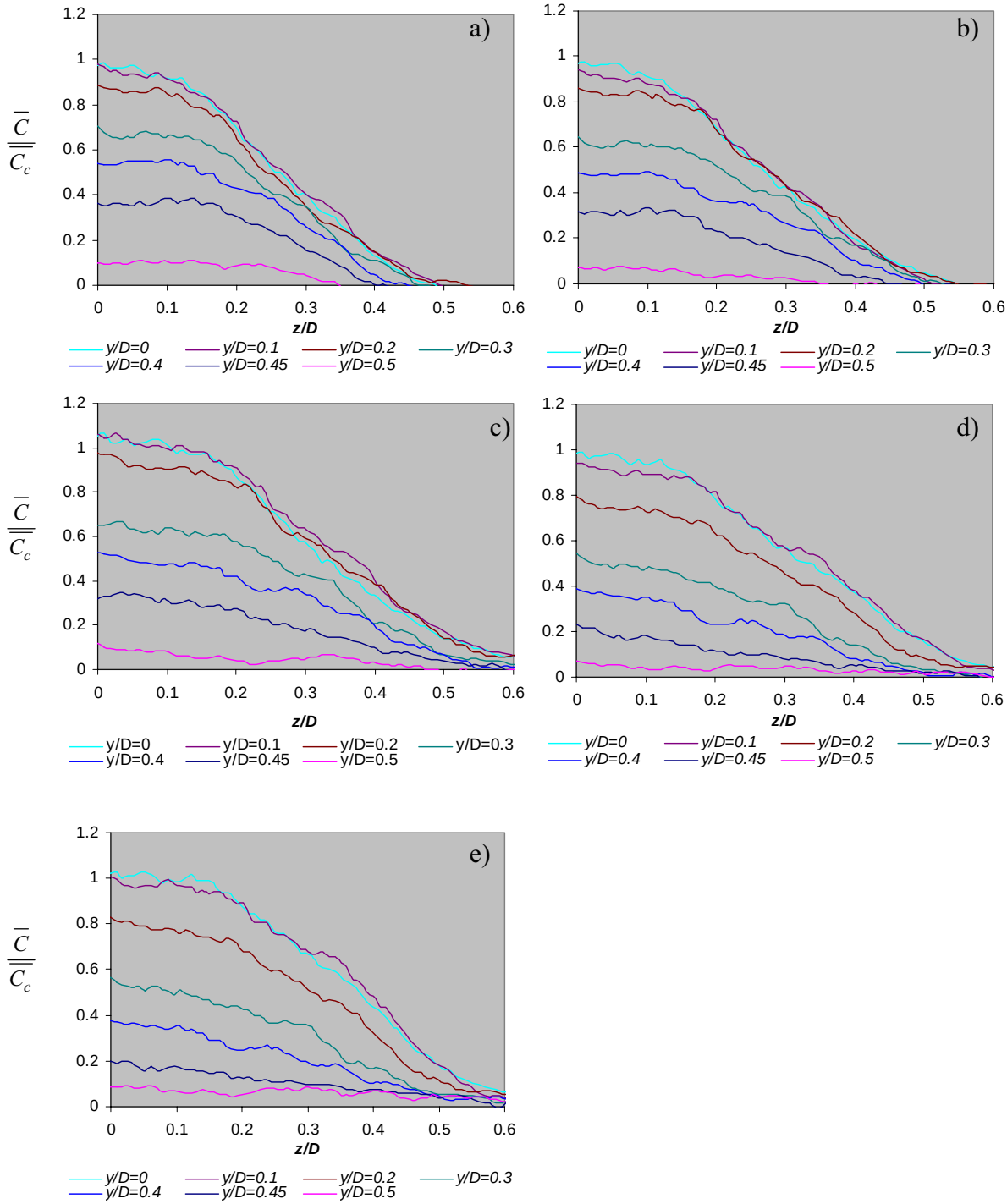

Figure B. 8: Normalised Concentration of the primary jet versus *z/D* through different *y/D* planes, at *x/D* =1, a) λ=0, b) λ=0.55, c) λ=1.4, d) λ=2.8, e) λ=3.6.

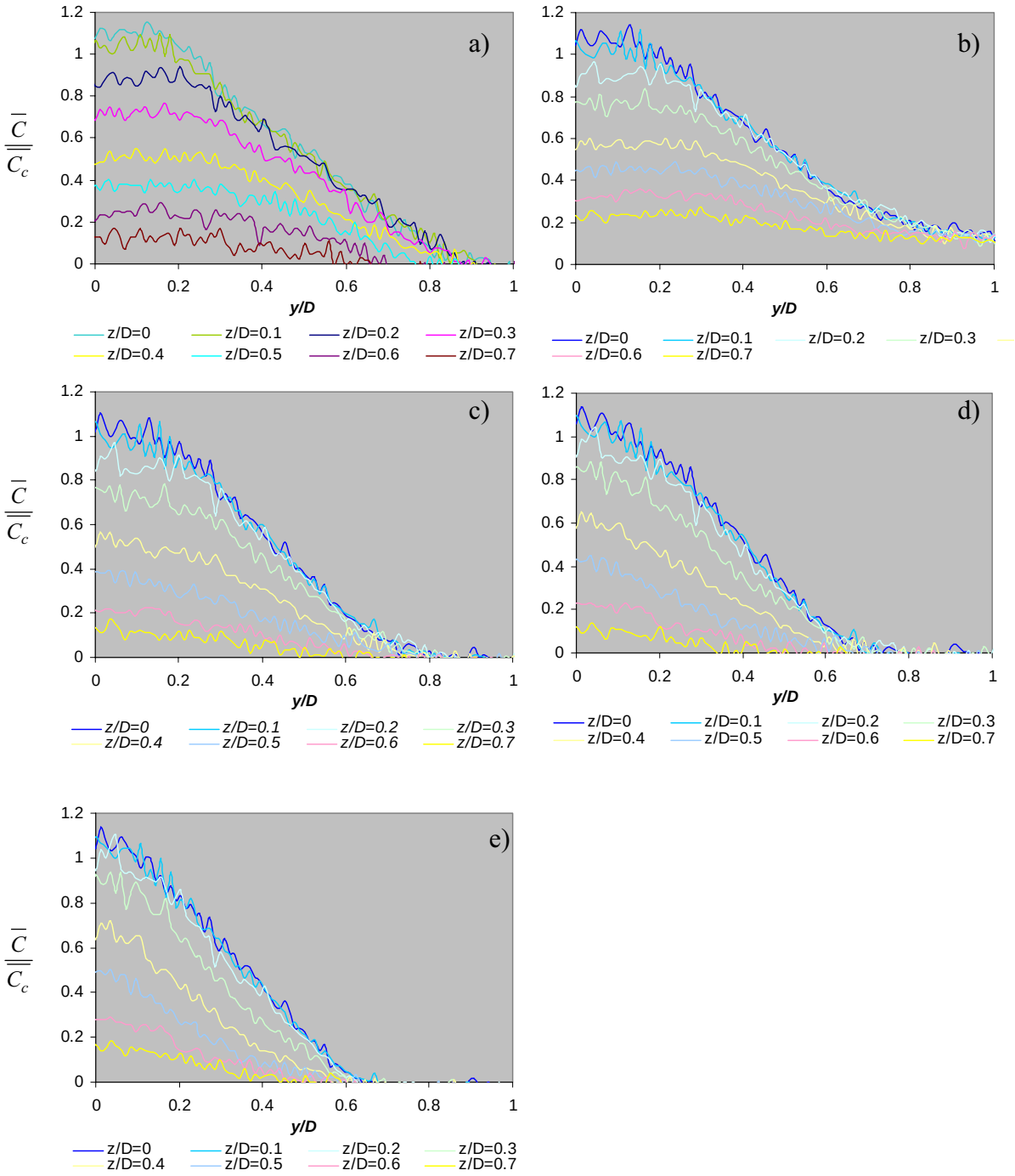

Figure B. 9: Normalised Concentration of the primary jet versus *y/D* through different *z/D* planes, at *x/D* =2, a) λ=0, b) λ=0.55, c) λ=1.4, d) λ=2.8, e) λ=3.6.

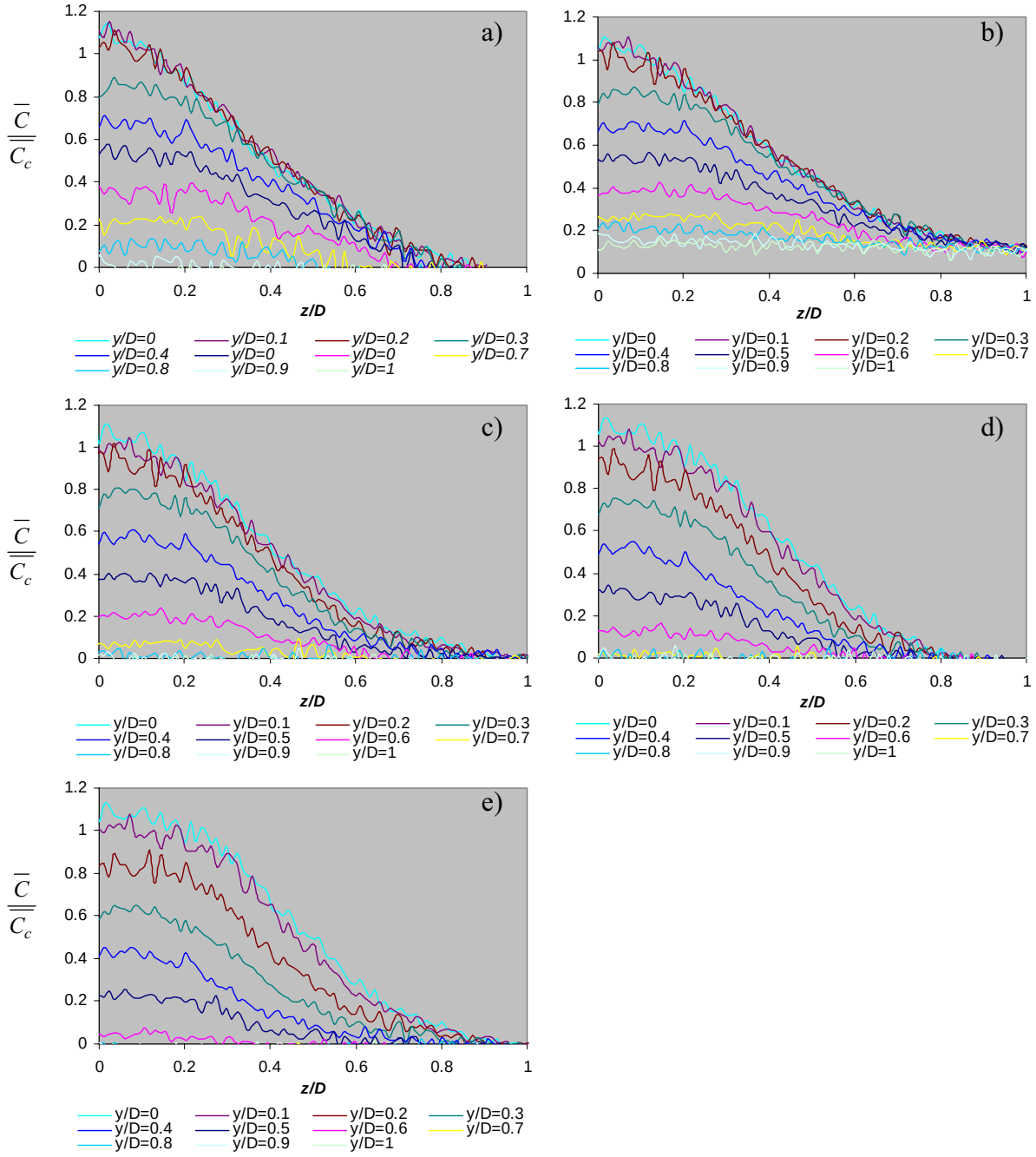

Figure B. 10: Normalised Concentration of the primary jet versus *z/D* through different *y/D* planes, at *x/D* =2, a) λ=0, b) λ=0.55, c) λ=1.4, d) λ=2.8, e) λ=3.6.

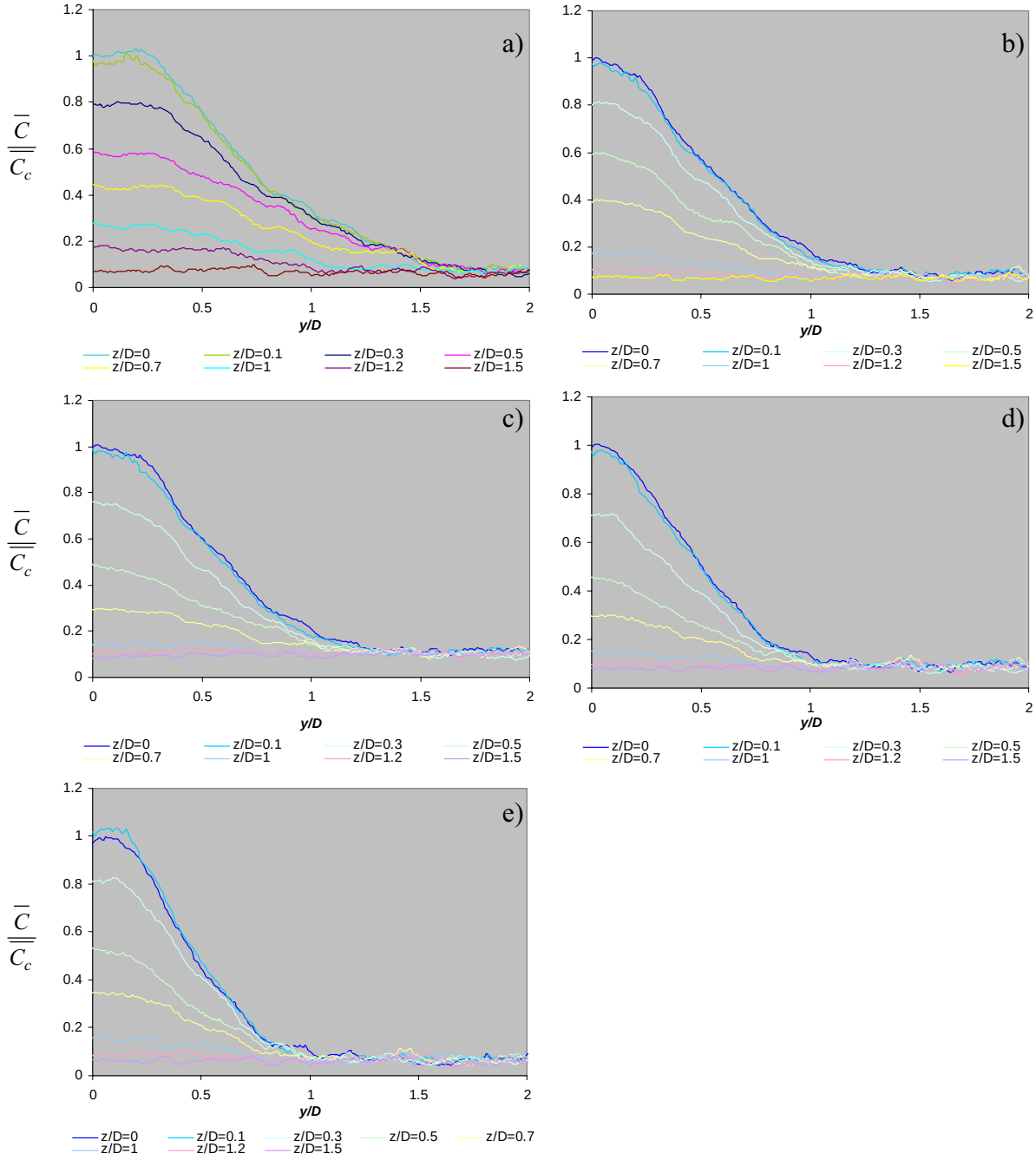

Figure B. 11: Normalised Concentration of the primary jet versus *y/D* through different *z/D* planes, at *x/D* =4, a) λ=0, b) λ=0.55, c) λ=1.4, d) λ=2.8, e) λ=3.6.

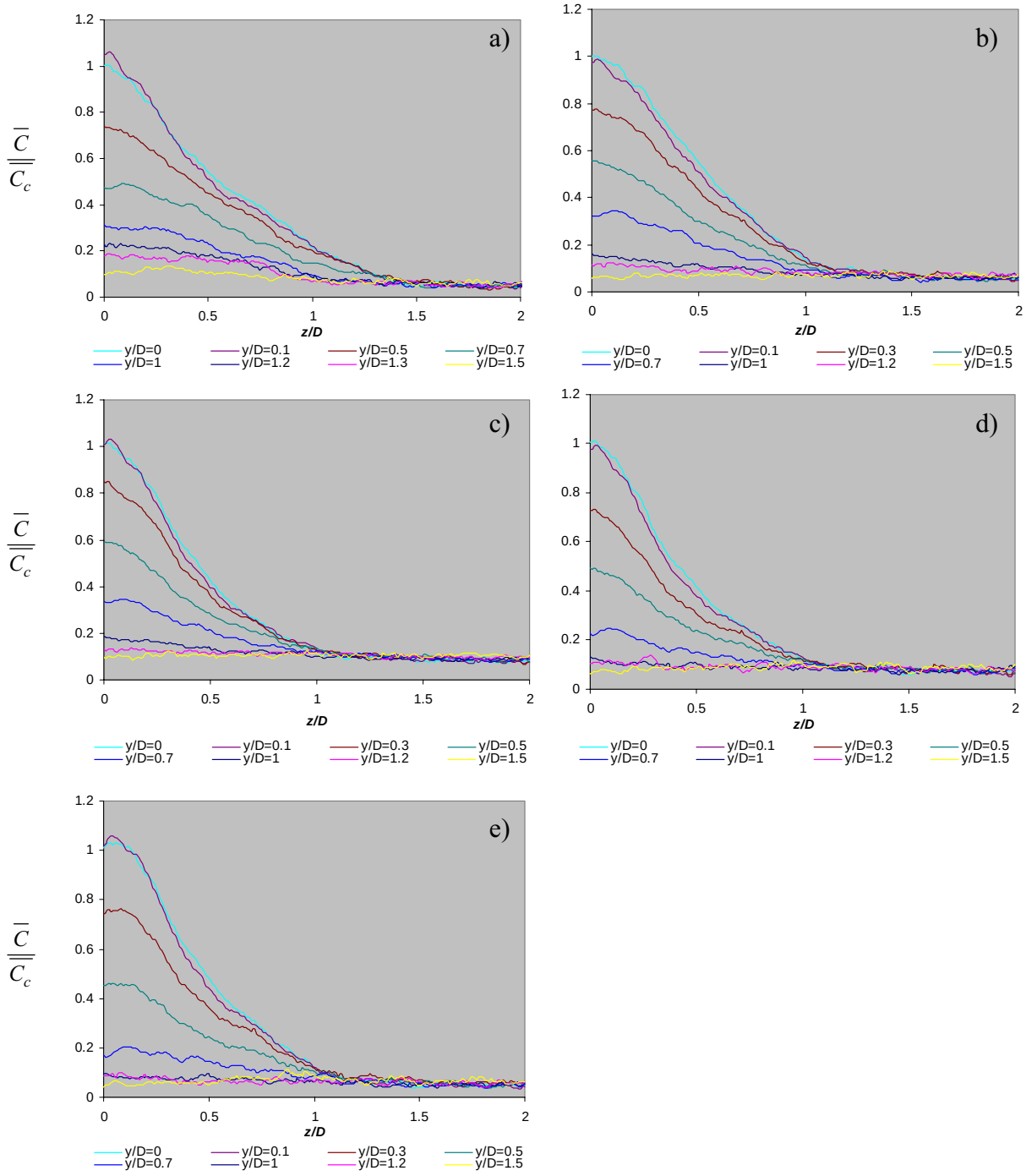

Figure B. 12: Normalised Concentration of the primary jet versus *z/D* through different *y/D* planes, at *x/D* =4, a) λ=0, b) λ=0.55, c) λ=1.4, d) λ=2.8, e) λ=3.6.

B.2 Secondary Jet Cross Stream Normalised Concentration

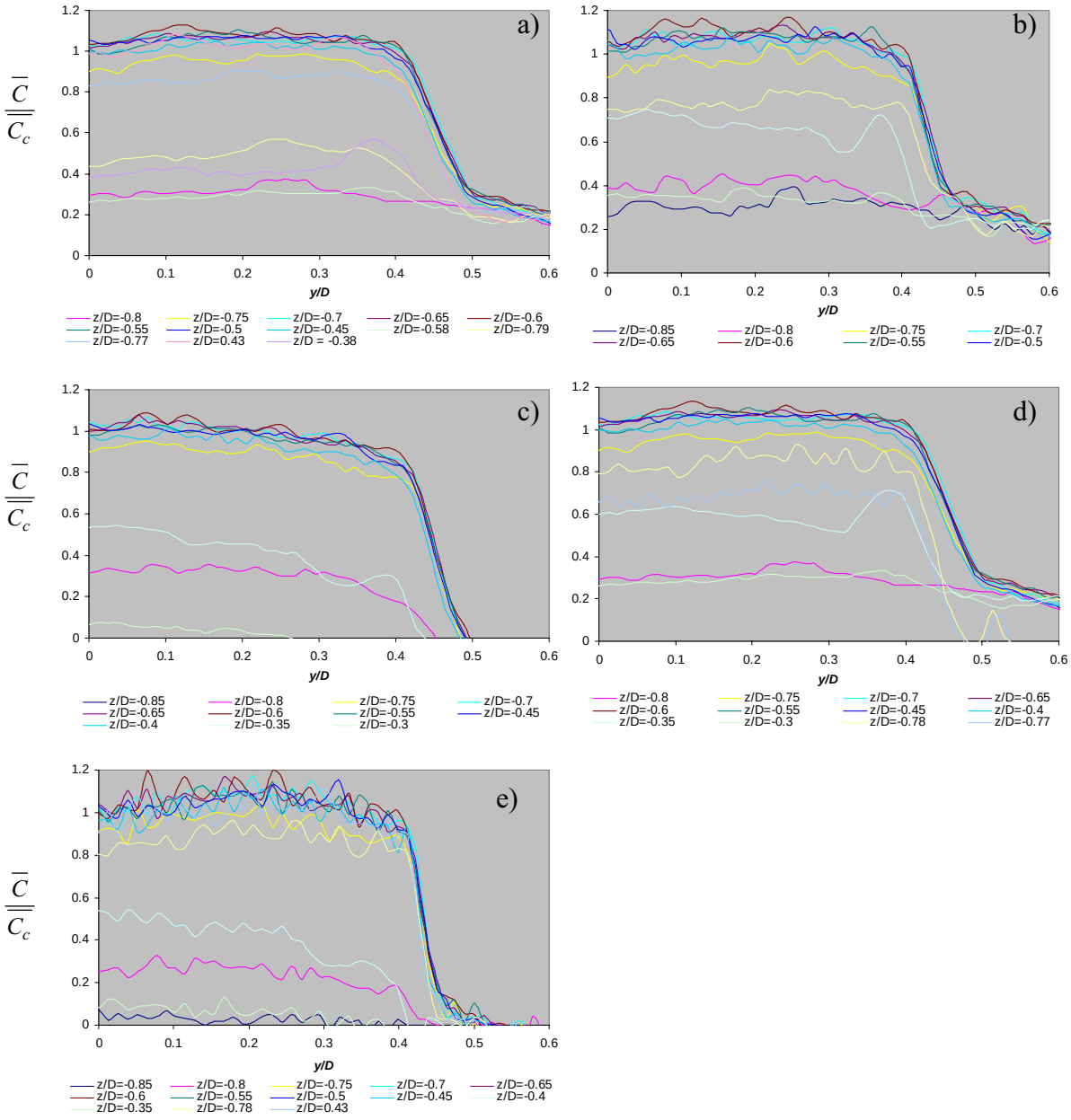

Figure B. 13: Normalised Concentration of the secondary jet versus *y/D* through different *z/D* planes, at *x/D* =0.1, a) λ=0.55, b) λ=1.4, c) λ=2.8, d) λ=3.6, e) λ=∞.

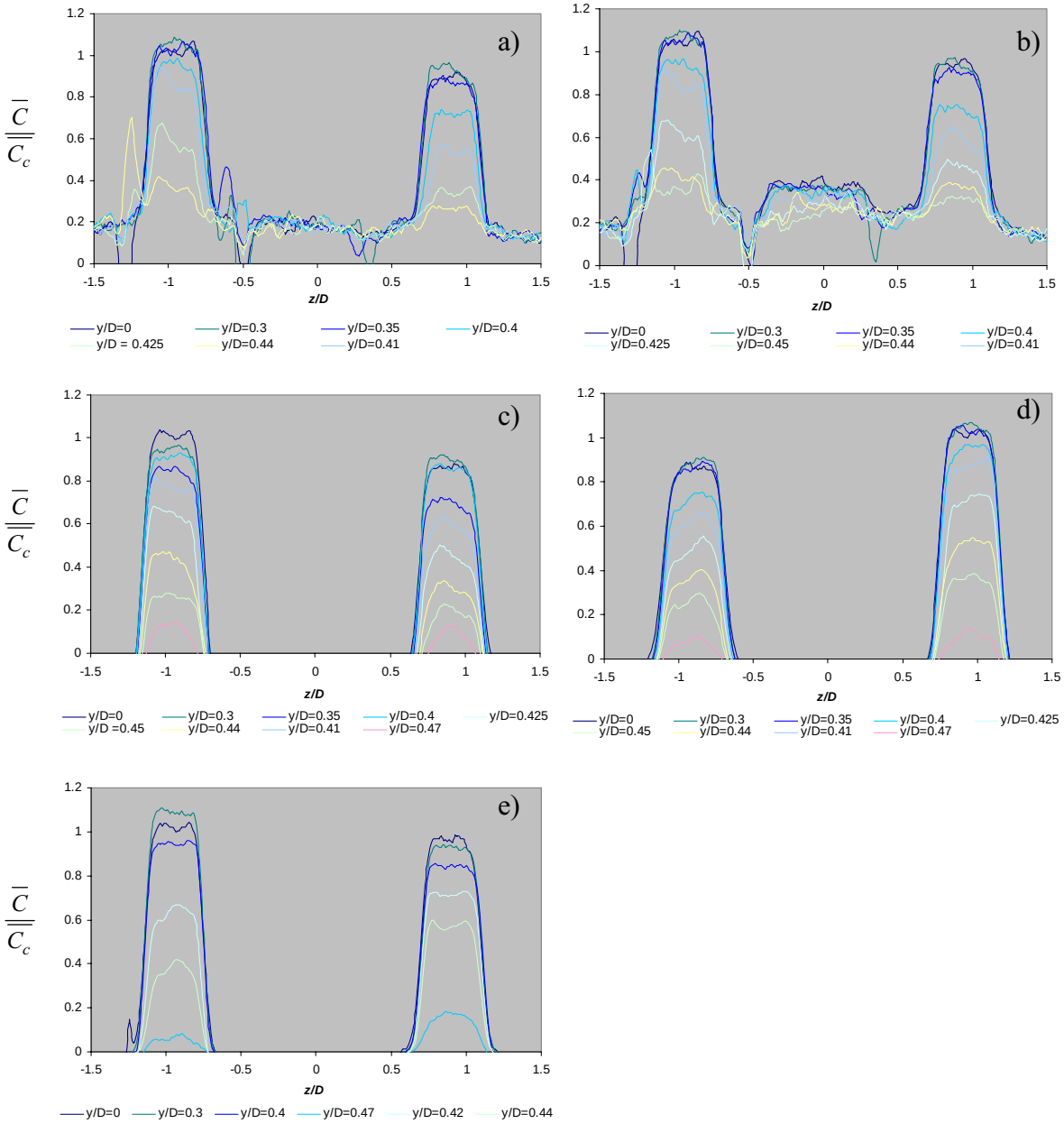

Figure B. 14: Normalised Concentration of the secondary jet versus *z/D* through different *y/D* planes, at *x/D* =0.1, a) λ=0.55, b) λ=1.4, c) λ=2.8, d) λ=3.6, e) λ=∞.

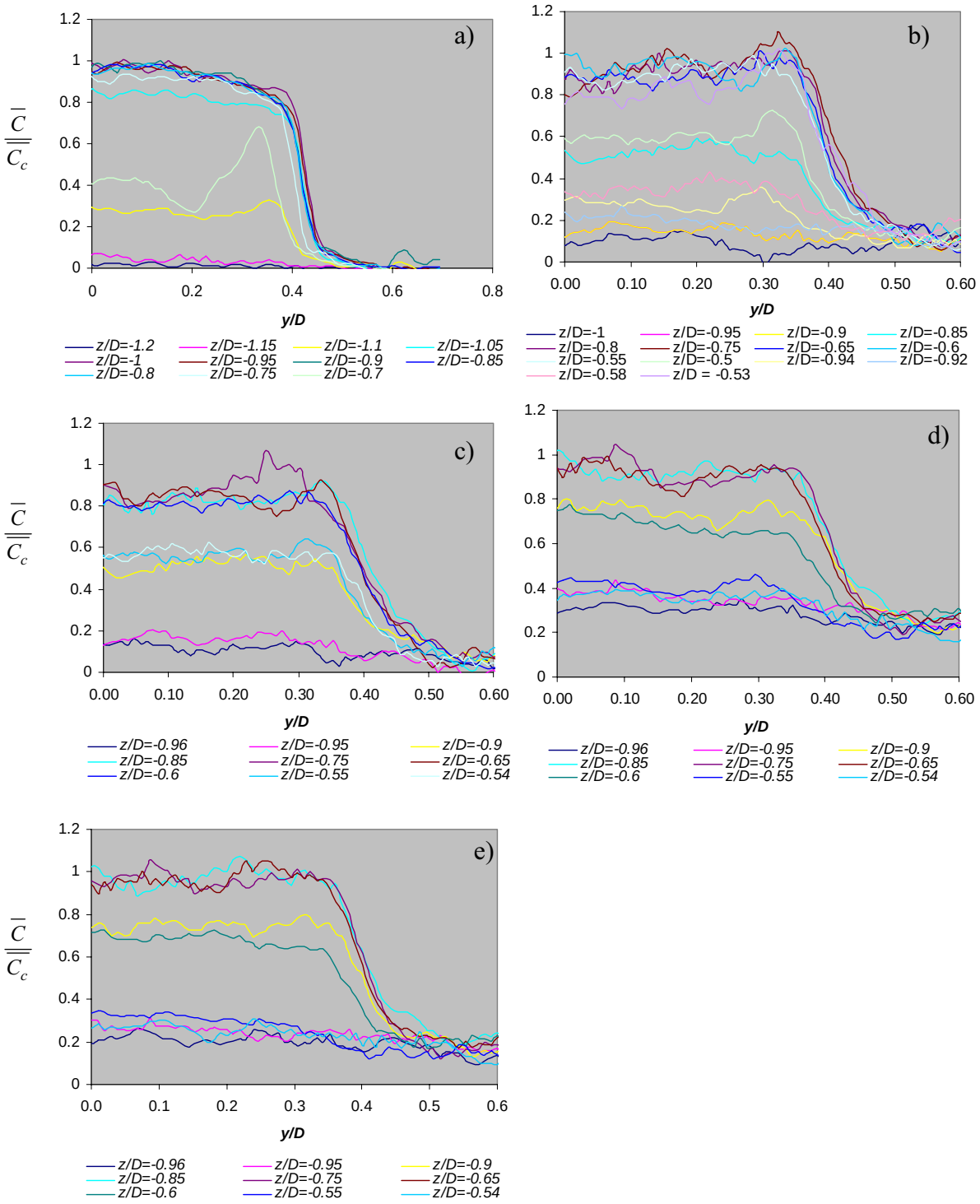

Figure B. 15: Normalised Concentration of the secondary jet versus *y/D* through different *z/D* planes, at *x/D* =0.2, a) λ=0.55, b) λ=1.4, c) λ=2.8, d) λ=3.6, e) λ=∞.

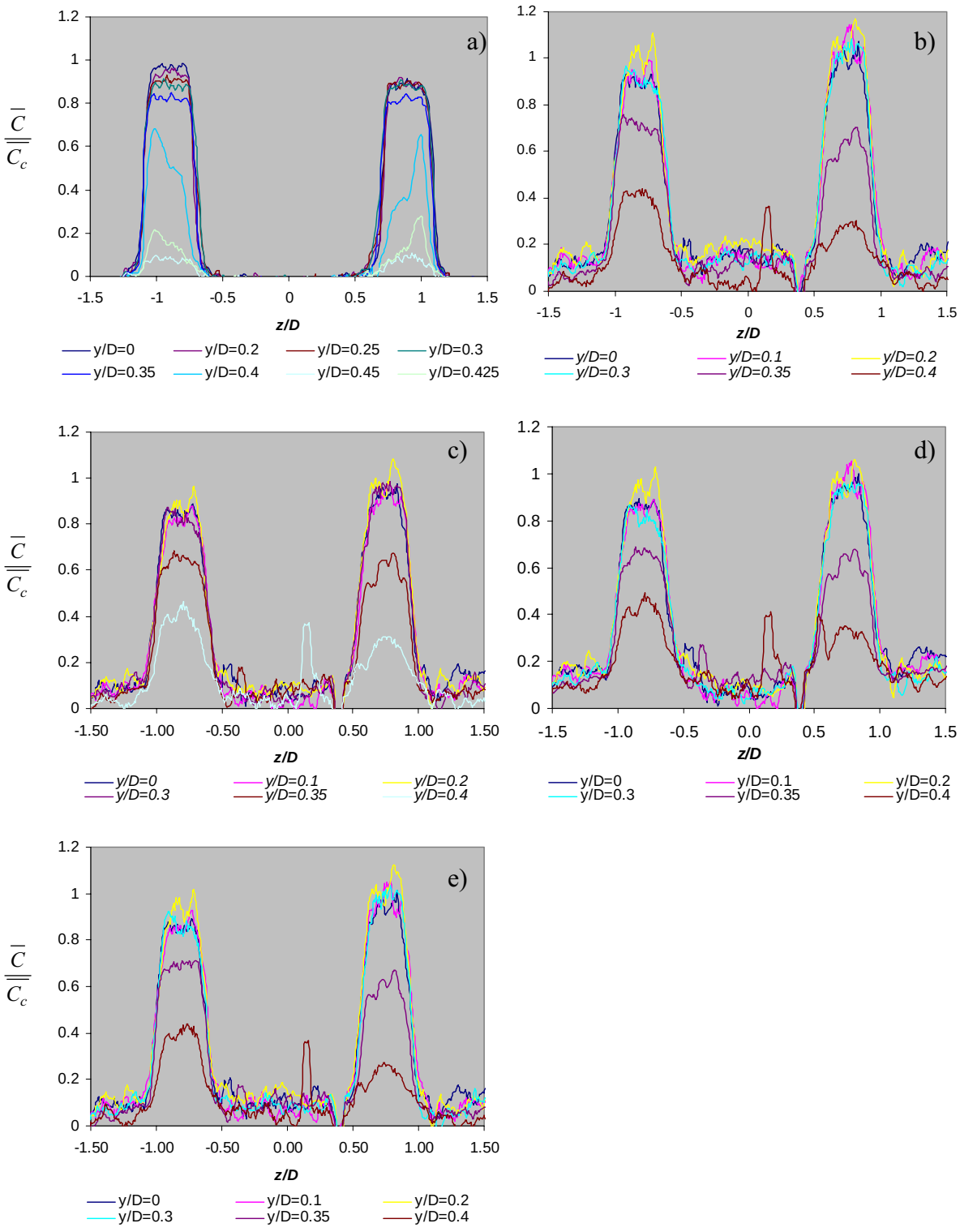

Figure B. 16: Normalised Concentration of the secondary jet versus *z/D* through different *y/D* planes, at *x/D* =0.2, a) λ=0.55, b) λ=1.4, c) λ=2.8, d) λ=3.6, e) λ=∞.

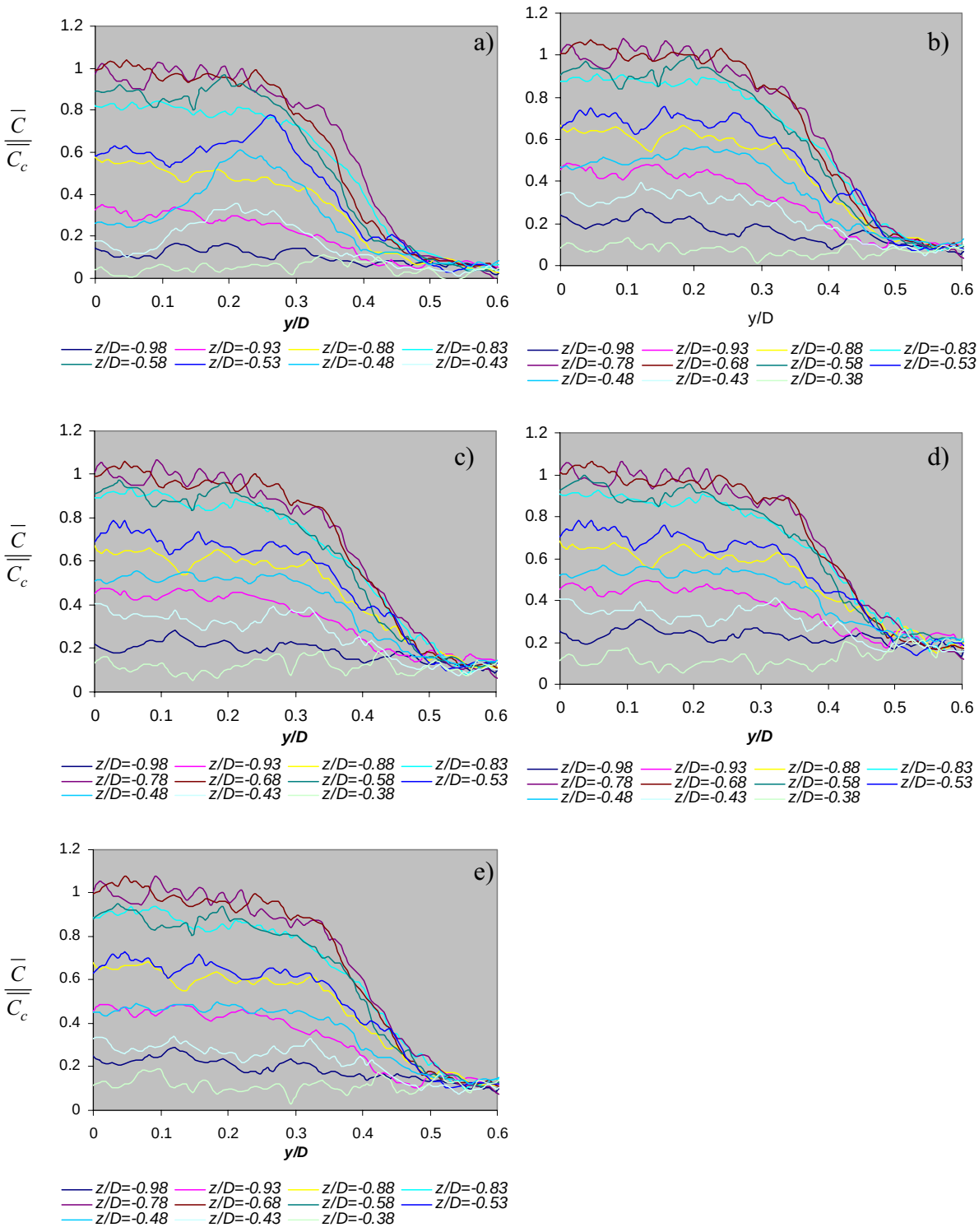

Figure B. 17: Normalised Concentration of the secondary jet versus *z/D* through different *y/D* planes, at *x/D* =0.5, a) λ=0.55, b) λ=1.4, c) λ=2.8, d) λ=3.6, e) λ=∞.

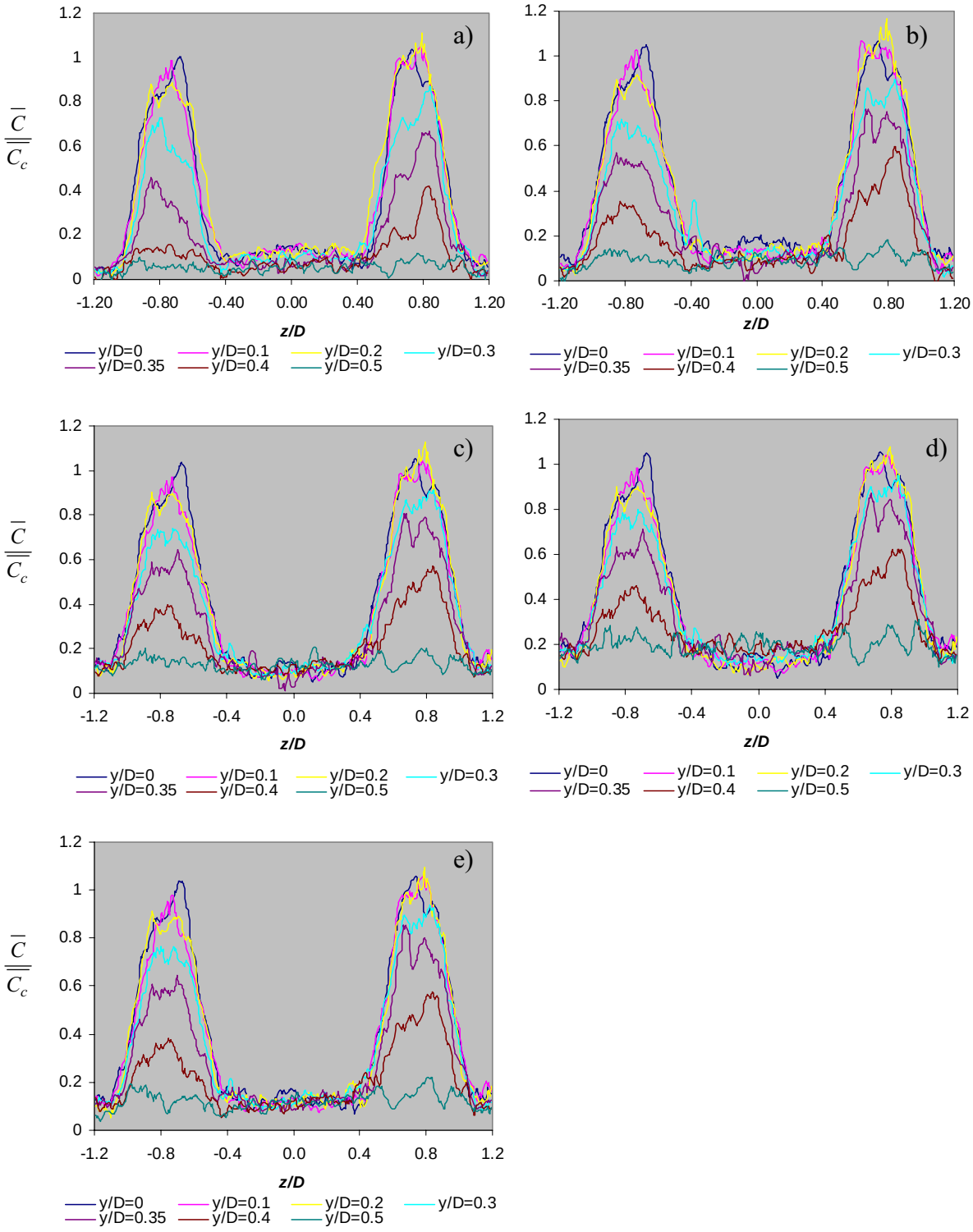

Figure B. 18: Normalised Concentration of the secondary jet versus *z/D* through different *y/D* planes, at *x/D* =0.5, a) λ=0.55, b) λ=1.4, c) λ=2.8, d) λ=3.6, e) λ=∞.

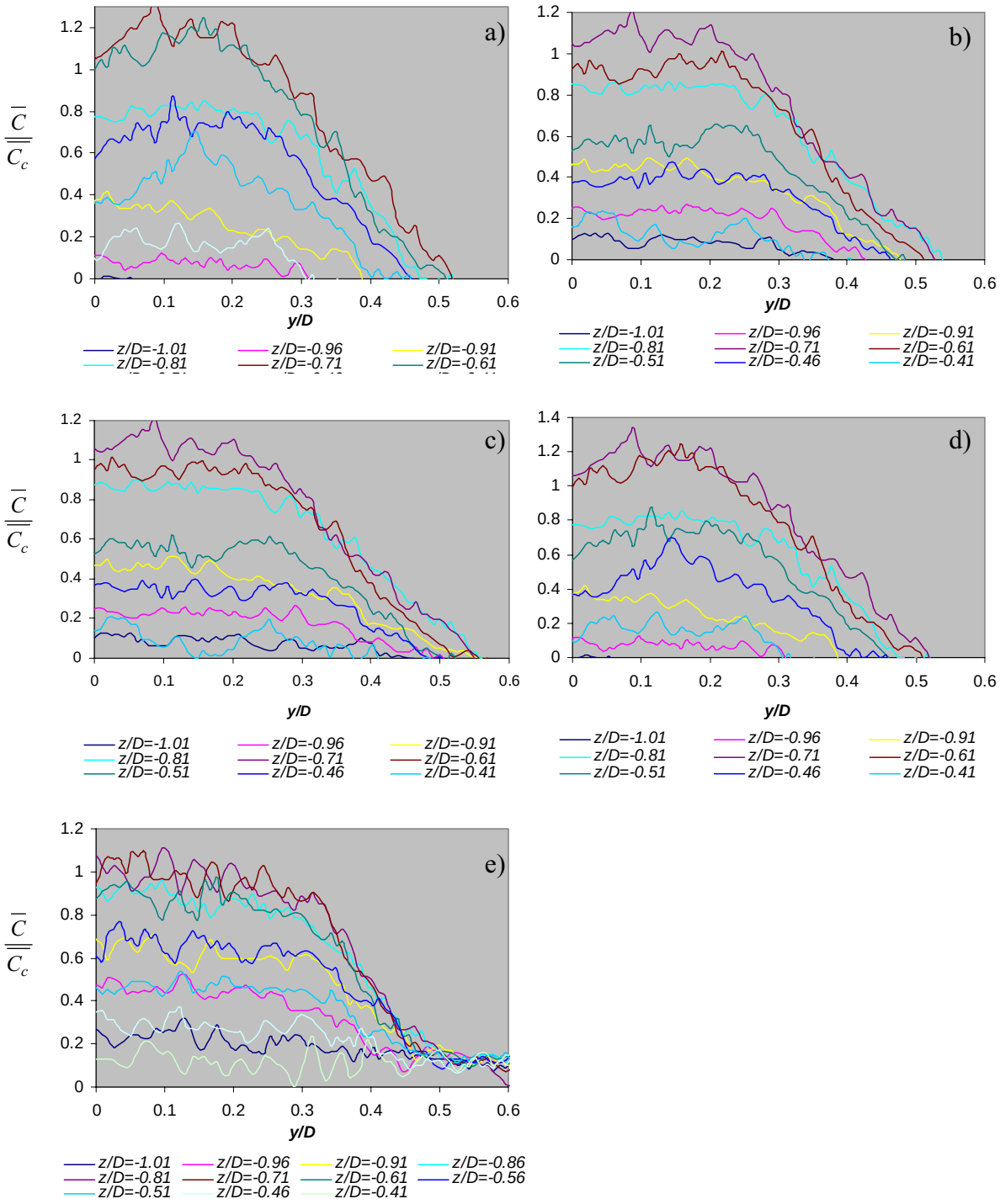

Figure B. 19: Normalised Concentration of the secondary jet versus *y/D* through different *z/D* planes, at *x/D* =1, a) λ=0.55, b) λ=1.4, c) λ=2.8, d) λ=3.6, e) λ=∞.

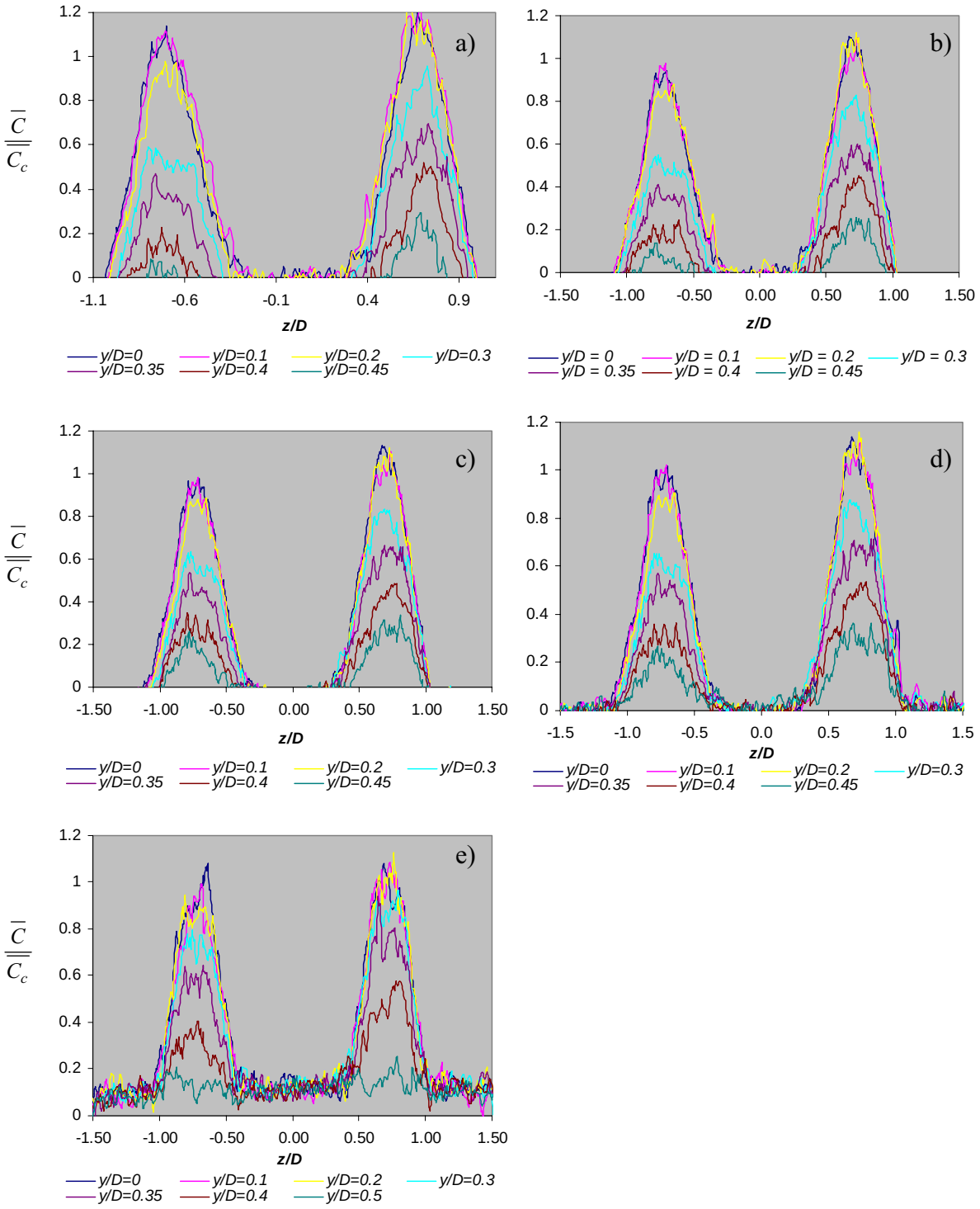

Figure B. 20: Normalised Concentration of the secondary jet versus *z/D* through different *y/D* planes, at *x/D* =1, a) λ=0.55, b) λ=1.4, c) λ=2.8, d) λ=3.6, e) λ=∞.

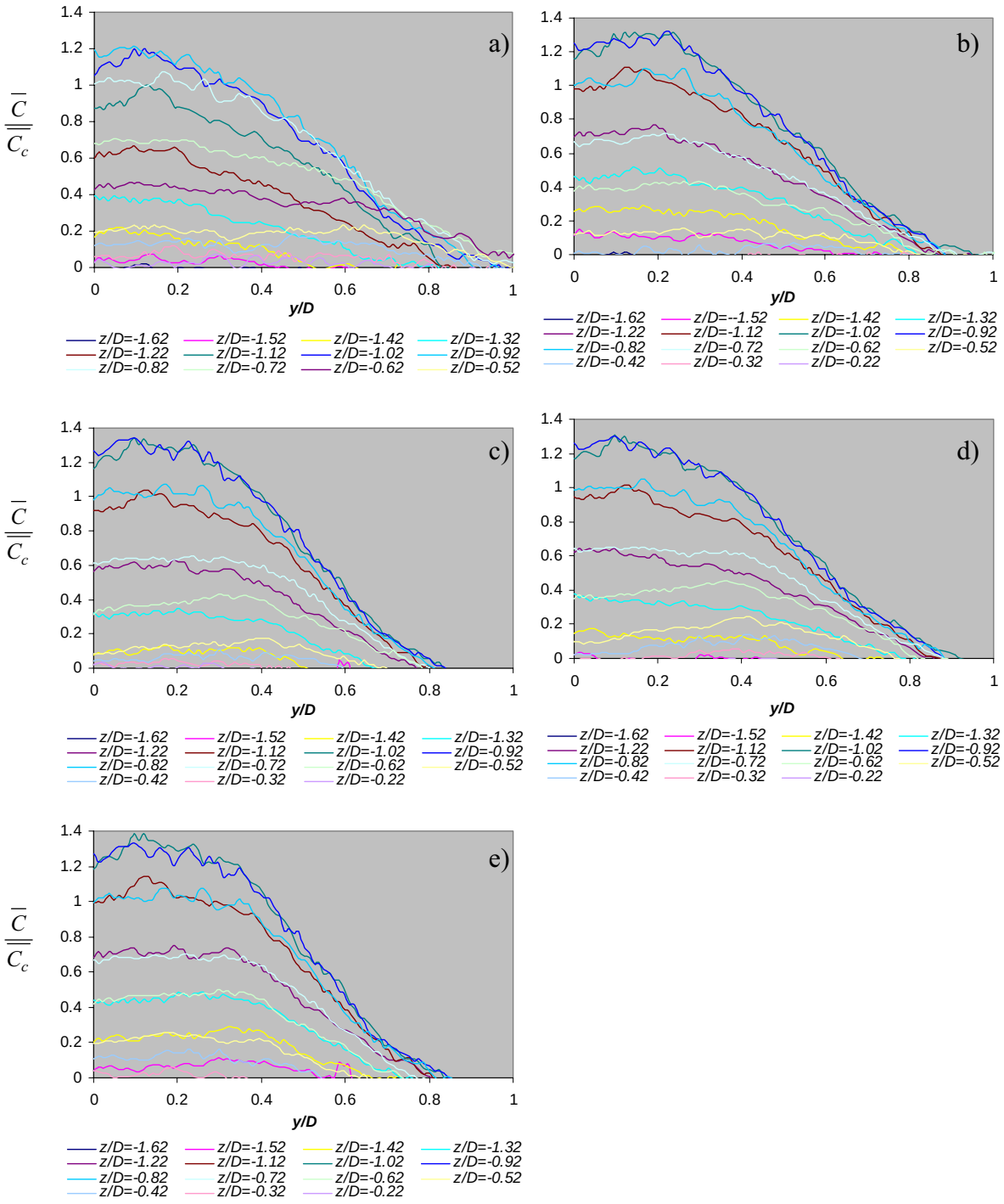

Figure B. 21: Normalised Concentration of the secondary jet versus *y/D* through different *z/D* planes, at *x/D* =2, a) λ=0.55, b) λ=1.4, c) λ=2.8, d) λ=3.6, e) λ=∞.

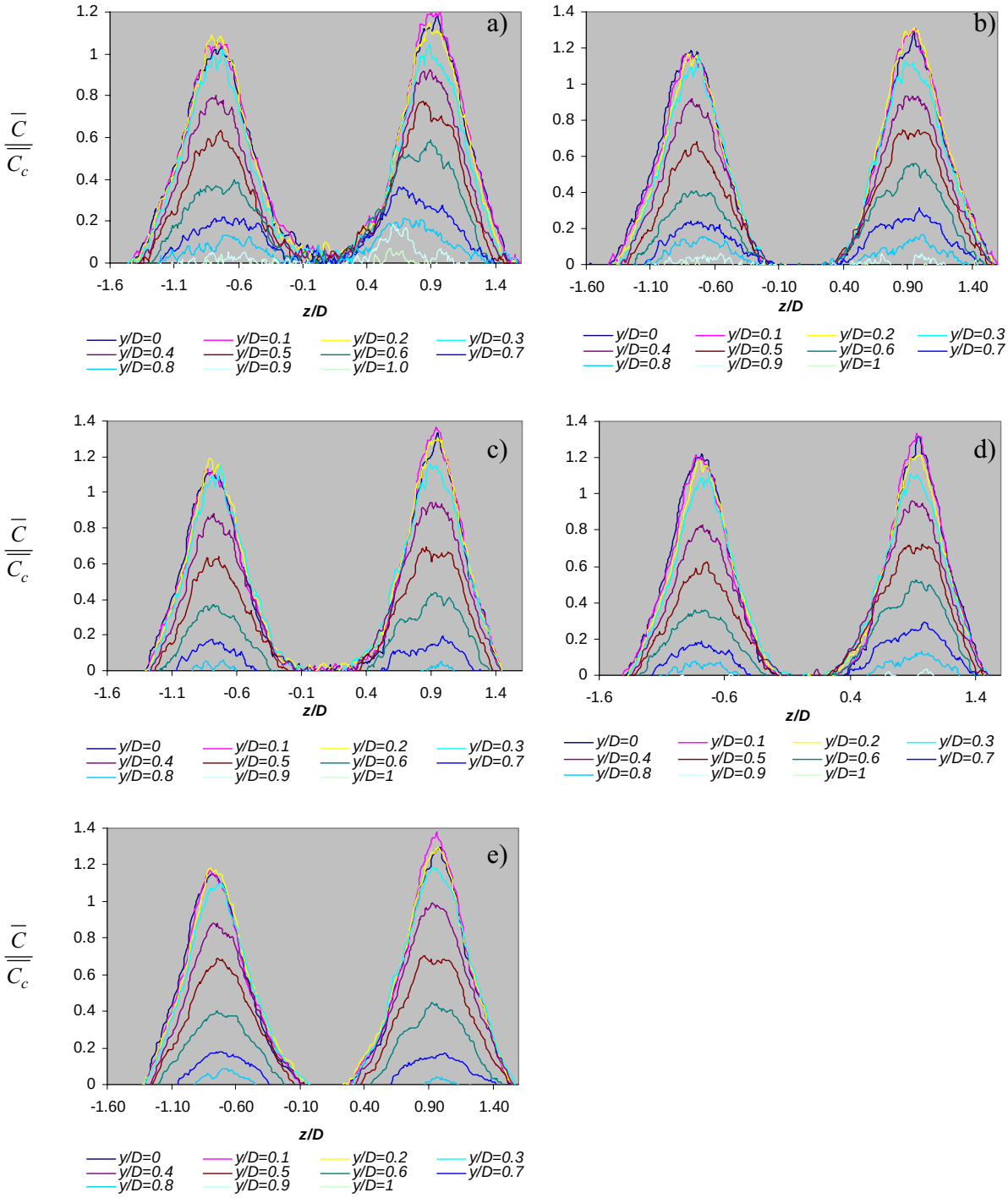

Figure B. 22: Normalised Concentration of the secondary jet versus *z/D* through different *y/D* planes, at *x/D* =2, a) λ=0.55, b) λ=1.4, c) λ=2.8, d) λ=3.6, e) λ=∞.

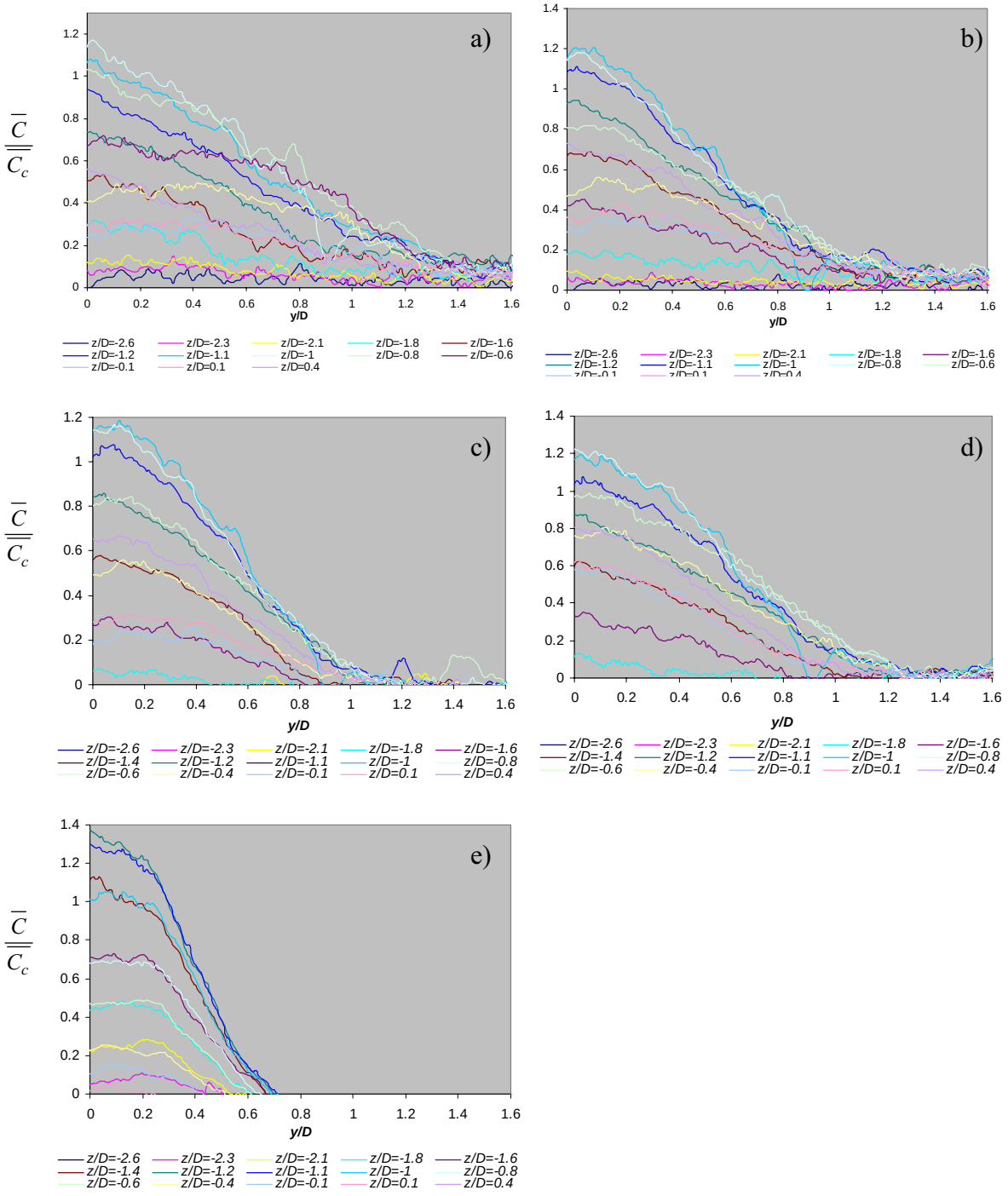

Figure B. 23: Normalised Concentration of the secondary jet versus *y/D* through different *z/D* planes, at *x/D* =4, a) λ=0.55, b) λ=1.4, c) λ=2.8, d) λ=3.6, e) λ=∞.

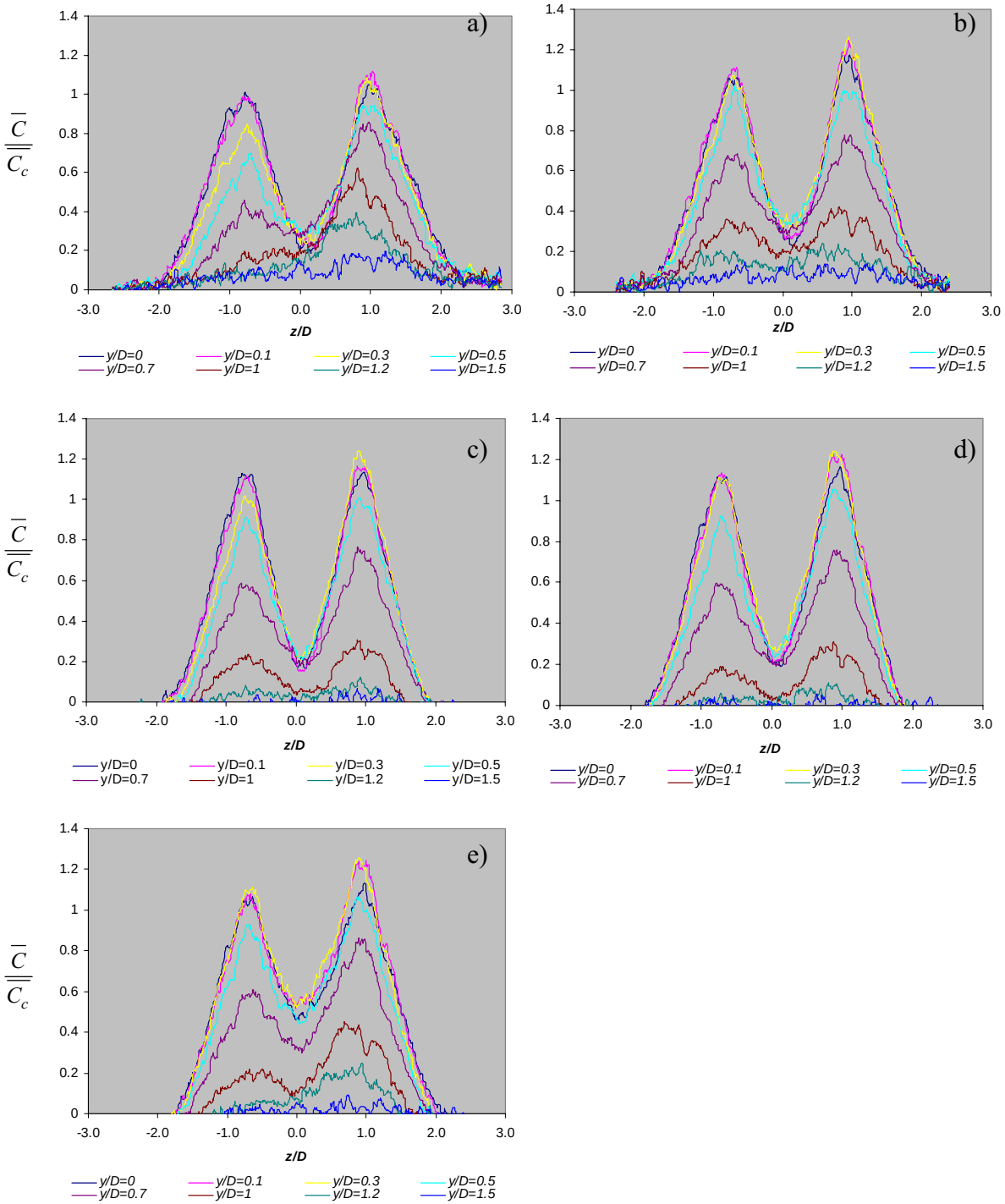

Figure B. 24: Normalised Concentration of the secondary jet versus *z/D* through different *y/D* planes, at *x/D* =4, a) λ=0.55, b) λ=1.4, c) λ=2.8, d) λ=3.6, e) λ=∞.

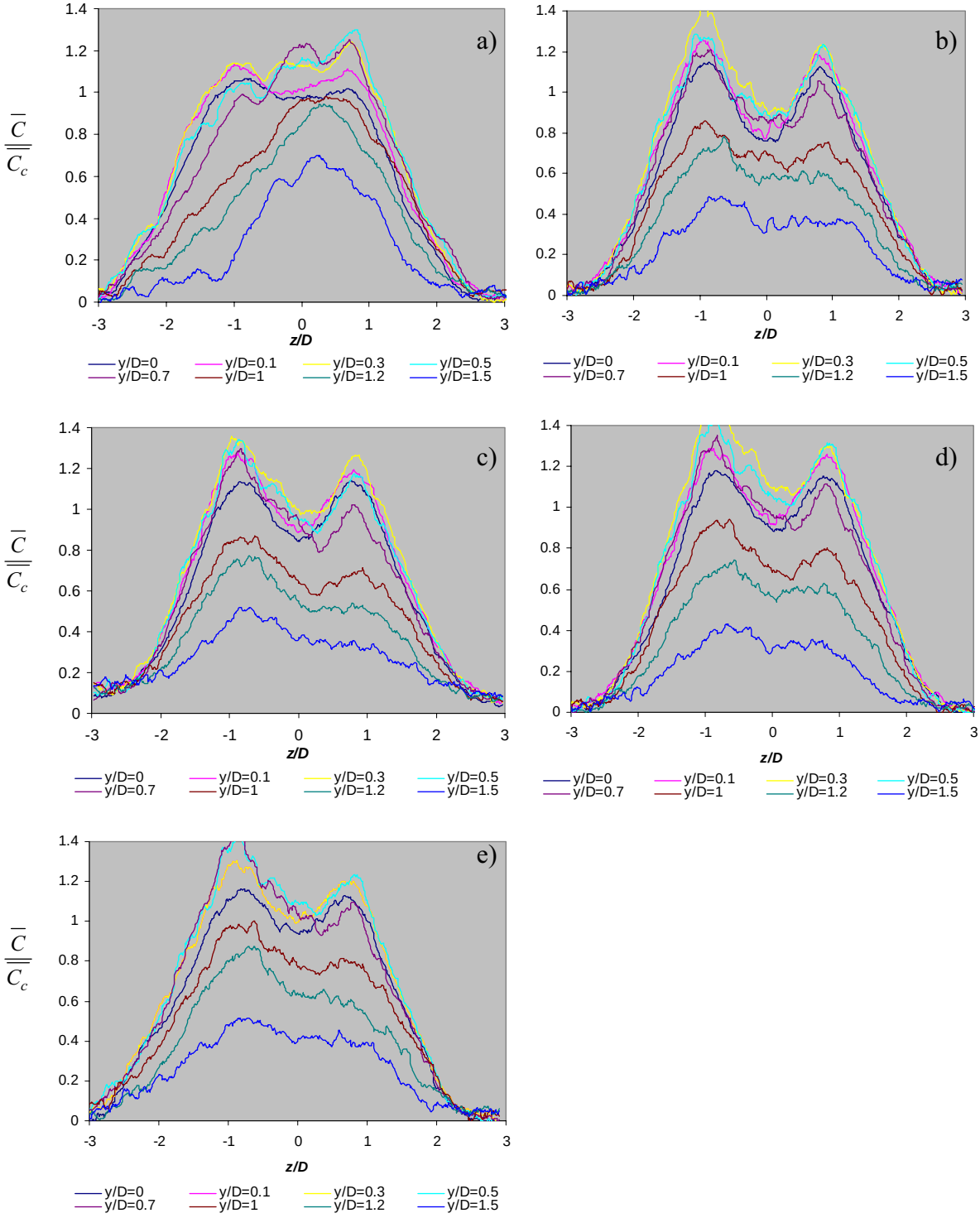

Figure B. 25: Normalised Concentration of the secondary jet versus *z/D* through different *y/D* planes, at *x/D* =6, a) λ=0.55, b) λ=1.4, c) λ=2.8, d) λ=3.6, e) λ=∞.

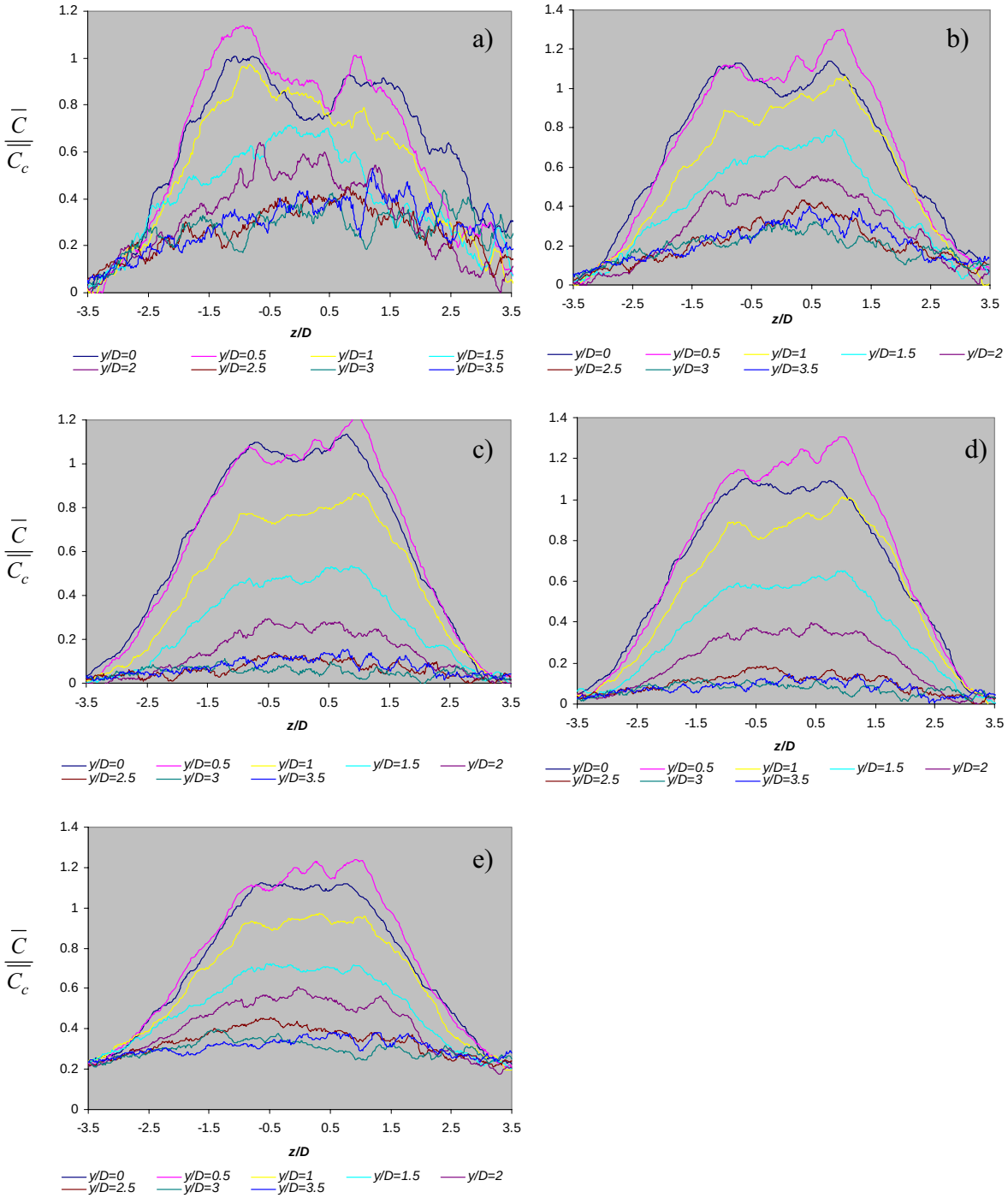

Figure B. 26: Normalised Concentration of the secondary jet versus *z/D* through different *y/D* planes, at *x/D* =8, a) λ=0.55, b) λ=1.4, c) λ=2.8, d) λ=3.6, e) λ=∞.